Approximate periodically focused solutions to the nonlinear Vlasov-Maxwell equations for intense beam propagation through an alternating-gradient field configuration

Ronald C. Davidson and Hong Qin
Plasma Physics Laboratory, Princeton University, Princeton, New Jersey 08543

Paul J. Channell
Los Alamos National Laboratory, Los Alamos, New Mexico 87545
(Received 12 January 1999; published 28 July 1999)

This paper considers an intense non-neutral ion beam propagating in the z direction through a periodic-focusing quadrupole or solenoidal field with transverse focusing force, $-[\kappa_x(s)x\hat{\mathbf{e}}_x + \kappa_y(s)y\hat{\mathbf{e}}_y]$, on the beam ions. Here, $s = \beta_b ct$ is the axial coordinate, $(\gamma_b - 1)m_b c^2$ is the directed axial kinetic energy of the beam ions, and the (oscillatory) lattice coefficients satisfy $\kappa_x(s + S) = \kappa_x(s)$ and $\kappa_y(s + S) = \kappa_y(s)$, where $S =$ const is the periodicity length of the focusing field. The theoretical model employs the Vlasov-Maxwell equations to describe the nonlinear evolution of the distribution function $f_b(x, y, x', y', s)$ and the (normalized) self-field potential $\psi(x, y, s)$ in the transverse laboratory-frame phase space (x, y, x', y'). Here, $\hat{H}(x, y, x', y', s) = (1/2)(x'^2 + y'^2) + (1/2)[\kappa_x(s)x^2 + \kappa_y(s)y^2] + \psi(x, y, s)$ is the (dimensionless) Hamiltonian for particle motion in the applied field plus self-field configurations, where (x, y) and (x', y') are the transverse displacement and velocity components, respectively, and $\psi(x, y, s)$ is the self-field potential. The Hamiltonian is formally assumed to be of order ϵ, a small dimensionless parameter proportional to the characteristic strength of the focusing field as measured by the lattice coefficients $\kappa_x(s)$ and $\kappa_y(s)$. Using a third-order Hamiltonian averaging technique developed by P. J. Channell [Phys. Plasmas **6**, 982 (1999)], a canonical transformation is employed that utilizes an expanded generating function that transforms away the rapidly oscillating terms. This leads to a Hamiltonian, $\mathcal{H}(\tilde{X}, \tilde{Y}, \tilde{X}', \tilde{Y}', s) = (1/2)(\tilde{X}'^2 + \tilde{Y}'^2) + (1/2)\kappa_f(\tilde{X}^2 + \tilde{Y}^2) + \psi(\tilde{X}, \tilde{Y}, s)$, correct to order ϵ^3 in the "slow" transformed variables $(\tilde{X}, \tilde{Y}, \tilde{X}', \tilde{Y}')$. Here, the transverse focusing coefficient in the transformed variables satisfies $\kappa_f =$ const, and the asymptotic expansion procedure is expected to be valid for a sufficiently small phase advance ($\sigma < \pi/3 = 60°$, say). Properties of axisymmetric beam equilibrium distribution functions, $F_b^0(\mathcal{H}^0)$, with $\partial/\partial s = 0 = \partial/\partial\Theta$, are calculated in the transformed variables, and the results are transformed back to the laboratory frame. Corresponding properties of the *periodically focused* distribution function $f_b(x, y, x', y', s)$ are calculated correct to order ϵ^3 in the laboratory frame, including statistical averages such as the mean-square beam dimensions, $\langle x^2\rangle(s)$ and $\langle y^2\rangle(s)$, the unnormalized transverse beam emittances, $\epsilon_x(s)$ and $\epsilon_y(s)$, the self-field potential, $\psi(x, y, s)$, the number density of beam particles, $n_b(x, y, s)$, and the transverse flow velocity, $\mathbf{V}_b(x, y, s)$. As expected, the beam cross section in the laboratory frame is a pulsating ellipse for the case of a periodic-focusing quadrupole field or a pulsating circular cross section for the case of a periodic-focusing solenoidal field.

PACS numbers: 29.27.Bd, 41.75.–i, 41.85.–p

I. INTRODUCTION

Periodic focusing accelerators and transport systems [1–5] have a wide range of applications ranging from basic scientific research to applications such as heavy ion fusion, tritium production, spallation neutron sources, and nuclear waste treatment, to mention a few examples [6–9]. Of particular interest, at the high beam currents and charge densities of practical interest, are the combined effects of the applied focusing field and the intense self-fields produced by the beam space charge and current on determining detailed equilibrium, stability, and transport properties [1]. Through analytical studies based on the nonlinear Vlasov-Maxwell equations, and numerical simulations using particle-in-cell models and nonlinear perturbative simulation techniques, considerable progress has been made in developing an improved understanding of the collective processes and nonlinear beam dynamics characteristic of high-intensity beam propagation in periodic-focusing and uniform-focusing transport systems [10–33]. However, despite the extensive literature on intense beam equilibrium and stability properties, until the present paper, the Kapchinskij-Vladimirskij (KV) beam equilibrium [10,11], including its recent generalization to a rotating beam in a periodic-focusing solenoidal field [21–23], has been the *only* known periodically focused equilibrium solution to the nonlinear Vlasov-Maxwell equations for an intense beam propagating through an alternating-gradient quadrupole or solenoidal field configuration. While allowing for high space-charge intensity, the KV distribution is nonetheless of very limited practical interest, particularly because the (monoenergetic) distribution function has a *highly-inverted* (and unphysical) distribution in phase space and the corresponding density profile is *exactly uniform* in the beam interior.

It is, therefore, very important to develop a framework based on the nonlinear Vlasov-Maxwell equations [12,21] that is able to investigate the equilibrium and stability properties of a far more general class of periodically focused beam distribution functions. In a recent calculation [34], Channell has developed a third-order Hamiltonian averaging technique for investigating solutions to the nonlinear Vlasov-Maxwell equations for systems subject to a periodic external force. Following the Von Zeipel procedure, the formalism [34] uses a canonical transformation given by an expanded generating function to transform away the rapidly oscillating terms [35–38] and end up with a Hamiltonian $\mathcal{H}$ that depends only on "slow" variables. The purpose of the present analysis is to apply this averaging technique to intense beam propagation through a periodic-focusing lattice. The asymptotic expansion procedure is expected to be valid [34] for sufficiently small phase advance ($\sigma \lesssim 60°$, say).

To briefly summarize, the present analysis considers a high-intensity non-neutral beam of positive ions (with charge $+Z_b e$ and rest mass m_b) propagating in the z direction with characteristic average axial momentum $\gamma_b m_b \beta_b c$ and directed kinetic energy $(\gamma_b - 1)m_b c^2$. The beam propagates through an applied field that produces a transverse focusing force, $-[\kappa_x(s)x\hat{\mathbf{e}}_x + \kappa_y(s)y\hat{\mathbf{e}}_y]$, on the beam particles. Here, $V_b = \beta_b c = \text{const}$ is the average axial velocity, $\gamma_b = (1 - \beta_b^2)^{-1/2}$ is the relative mass factor, c is the speed of light *in vacuo*, $s = \beta_b ct$ is the axial coordinate, the ion motion in the beam frame is assumed to be nonrelativistic, and the lattice functions, $\kappa_x(s)$ and $\kappa_y(s)$, have axial periodicity length $S = \text{const}$. Both the cases of a periodic-focusing quadrupole field [Eq. (9)] and a periodic-focusing solenoidal field [Eq. (11)] are considered in the present analysis. Furthermore, the analysis assumes negligible axial momentum spread, and the starting point is the nonlinear Vlasov-Maxwell equations (3) and (4) for the distribution function $f_b(x,y,x',y',s)$ and (normalized) self-field potential $\psi(x,y,s)$ in the transverse phase space (x,y,x',y') in the laboratory frame [12,21]. Here, the Hamiltonian for single-particle motion in the laboratory frame is given in dimensionless units by [Eq. (6)]

$$\hat{H}(x,y,x',y',s) = \frac{1}{2}(x'^2 + y'^2) + \frac{1}{2}[\kappa_x(s)x^2 + \kappa_y(s)y^2] + \psi(x,y,s),$$

where $\kappa_x(s + S) = \kappa_x(s)$ and $\kappa_y(s + S) = \kappa_y(s)$ are the (oscillating) lattice functions. The Hamiltonian $\hat{H}$ is formally assumed to be of order ϵ, a small dimensionless parameter proportional to the characteristic strength of the focusing field as measured by the lattice coefficients $\kappa_x(s)$ and $\kappa_y(s)$.

The organization of this paper is the following: The assumptions and theoretical model are summarized in Sec. II, including the nonlinear Vlasov-Maxwell equations for the distribution function $f_b(x,y,x',y',s)$ and self-field potential $\psi(x,y,s)$ in the laboratory frame. In Sec. III, we make use of Channell's third-order Hamiltonian averaging technique [34] to transform from laboratory-frame variables (x,y,x',y') to a new Hamiltonian $\mathcal{H}(\tilde{X},\tilde{Y},\tilde{X}',\tilde{Y}',s)$ in the slow variables $(\tilde{X},\tilde{Y},\tilde{X}',\tilde{Y}')$ correct to order ϵ^3. The formalism employs a canonical transformation given by an expanded generating function to transform away the rapidly oscillating terms [35–38]. This leads to a Hamiltonian in the transformed variables of the form [Eq. (79)]

$$\mathcal{H}(\tilde{X},\tilde{Y},\tilde{X}',\tilde{Y}',s) = \frac{1}{2}(\tilde{X}'^2 + \tilde{Y}'^2) + \frac{1}{2}\kappa_f(\tilde{X}^2 + \tilde{Y}^2) + \psi(\tilde{X},\tilde{Y},s),$$

where $\kappa_f = \text{const}$. Of course, an important by-product of the generating function analysis is the determination of the coordinate transformation that relates the laboratory-frame variables (x,y,x',y') to the slow variables $(\tilde{X},\tilde{Y},\tilde{X}',\tilde{Y}')$ [Eqs. (87)–(90)]. The major simplification associated with transforming to the slow variables $(\tilde{X},\tilde{Y},\tilde{X}',\tilde{Y}')$ is immediately evident from the expression for $\mathcal{H}(\tilde{X},\tilde{Y},\tilde{X}',\tilde{Y}',s)$. In particular, the focusing coefficient κ_f is both *constant* (independent of s) and *isotropic* in the transverse plane. This should be contrasted with the expression for the Hamiltonian $\hat{H}(x,y,x',y',s)$ in the laboratory frame, where the focusing coefficients $\kappa_x(s)$ and $\kappa_y(s)$ are rapidly oscillating functions of s. In Sec. IV, following a discussion of the nonlinear Vlasov-Maxwell equations for $F_b(\tilde{X},\tilde{Y},\tilde{X}',\tilde{Y}',s)$ and $\psi(\tilde{X},\tilde{Y},s)$ in the transformed variables, we present several examples of axisymmetric equilibrium solutions, i.e., distribution functions $F_b^0(\mathcal{H}^0)$ with $\partial/\partial s = 0$ and $\partial/\partial\Theta = 0$, corresponding to beam equilibria with circular cross sections in the transformed variables [12,21]. Of particular note is the class of distribution functions that satisfy $\partial F_b^0(\mathcal{H}^0)/\partial\mathcal{H}^0 \leq 0$, which can be shown to be *stable* [25,26]. Finally, in Sec. V, we exploit the inverse coordinate transformation, $\tilde{X}(x,y,x',y',s)$, $\tilde{Y}(x,y,x',y',s)$, etc., to determine properties of the *periodically focused* distribution function $f_b(x,y,s',y',s)$ in the laboratory frame correct to order ϵ^3, consistent with the class of constant-radius circular cross-section beam equilibria $F_b^0(\mathcal{H}^0)$ in the transformed variables. A wide range of important physical quantities are determined, including the distribution function $f_b(x,y,x',y',s)$; statistical averages such as the transverse mean-square beam dimensions, $\langle x^2\rangle(s)$ and $\langle y^2\rangle(s)$, and the unnormalized transverse emittances, $\epsilon_x(s)$ and $\epsilon_y(s)$; and macroscopic properties such as the number density of beam particles, $n_b(x,y,s) = \int dx'\, dy'\, f_b(x,y,x',y',s)$, and the self-field potential, $\psi(x,y,s)$, etc.

Finally, in the third-order averaging technique developed in Sec. III, it should be emphasized that the Hamiltonian is formally assumed to be of order ϵ, a small dimensionless parameter proportional to the characteristic strength of the focusing field [see Eqs. (6) and (15)] as measured by the lattice coefficients $\kappa_x(s)$ and $\kappa_y(s)$. To assure transverse confinement of the beam particles, the space-charge potential $\psi(x,y,s)$ in Eq. (6) is, of course, smaller than or comparable in size to the applied focusing potential, $(1/2)[\kappa_x(s)x^2 + \kappa_y(s)y^2]$, and the kinetic energy contribution, $(1/2)(x'^2 + y'^2)$, is allowed to be comparable in size to the applied focusing potential in the sense of a maximal ordering analysis. In this regard, treating the single-particle Hamiltonian to be of order $\epsilon \ll 1$, where ϵ is proportional to the focusing-field strength, is similar to the assumption made in standard analyses of the particle dynamics in intense charged particle beams at moderate values of phase advance [1–5]. For completeness, in Sec. V D we provide a semiquantitative estimate of the range of validity of the asymptotic analysis in Secs. III and IV by relating the small parameter ϵ to the focusing-field strength and the phase advance for the case of a sinusoidal quadrupole focusing lattice, $\kappa_q(s) = \hat{\kappa}_q \sin(2\pi s/S)$.

II. VLASOV-MAXWELL DESCRIPTION AND BASIC ASSUMPTIONS

In the present analysis, we consider a thin, intense non-neutral ion beam with characteristic radius r_b and average axial momentum $\gamma_b m_b \beta_b c$ propagating in the z direction through a periodic focusing field with axial periodicity length S. Here, $r_b \ll S$ is assumed, $(\gamma_b - 1)m_b c^2$ is the directed axial kinetic energy of the beam ions, $\gamma_b = (1-\beta_b^2)^{-1/2}$ is the relativistic mass factor, $V_b = \beta_b c$ is the average axial velocity, $+Z_b e$ and m_b are the ion charge and rest mass, respectively, and c is the speed of light *in vacuo*. The axial momentum spread of the beam ions is assumed to be negligibly small, and the ion motion in the beam frame is assumed to be nonrelativistic. We introduce the scaled time variable $s = \beta_b c t$ and the (dimensionless) transverse velocities $x' = dx/ds$ and $y' = dy/ds$. Then, within the context of the assumptions summarized above, the nonlinear beam dynamics in the transverse laboratory-frame phase space (x,y,x',y') is described self-consistently by the nonlinear Vlasov-Maxwell equations for the distribution function $f_b(x,y,x',y',s)$ and the normalized self-field potential $\psi(x,y,s) = Z_b e\phi(x,y,s)/\gamma_b^3 m_b \beta_b^2 c^2$, where $\phi(x,y,s)$ is the electrostatic potential. For a thin beam ($r_b \ll S$), we take the applied transverse focusing force on a beam particle to be of the form

$$\mathbf{F}_{\rm foc} = -[\kappa_x(s)x\hat{\mathbf{e}}_x + \kappa_y(s)y\hat{\mathbf{e}}_y], \tag{1}$$

where (x,y) is the transverse displacement from the beam axis and the s-dependent focusing coefficients satisfy

$$\kappa_x(s+S) = \kappa_x(s), \quad \kappa_y(s+S) = \kappa_y(s), \tag{2}$$

where $S = \text{const}$ is the axial periodicity length. The Vlasov-Maxwell equations for $f_b(x,y,x',y',s)$ and $\psi(x,y,s)$ can then be expressed as [12,21]

$$\left\{\frac{\partial}{\partial s} + x'\frac{\partial}{\partial x} + y'\frac{\partial}{\partial y} - \left[\kappa_x(s)x + \frac{\partial\psi}{\partial x}\right]\frac{\partial}{\partial x'} - \left[\kappa_y(s)y + \frac{\partial\psi}{\partial y}\right]\frac{\partial}{\partial y'}\right\} f_b = 0, \tag{3}$$

and

$$\left(\frac{\partial^2}{\partial x^2} + \frac{\partial^2}{\partial y^2}\right)\psi = -\frac{2\pi K_b}{N_b}\int dx'\, dy'\, f_b. \tag{4}$$

Here, $n_b(x,y,s) = \int dx'\, dy'\, f_b(x,y,x',y',s)$ is the number density of the beam ions, and the constants, K_b and N_b, are the self-field perveance and the number of beam ions per unit axial length, respectively, defined by

$$K_b = \frac{2N_b Z_b^2 e^2}{\gamma_b^3 m_b \beta_b^2 c^2} = \text{const}, \quad N_b = \int dx\, dy\, dx'\, dy'\, f_b = \text{const}. \tag{5}$$

The nonlinear Vlasov-Maxwell equations (3) and (4) can be used to investigate detailed beam propagation and stability properties [10–26] over a wide range of system parameters and choices of periodic lattice functions, $\kappa_x(s)$ and $\kappa_y(s)$. As a general remark, it is important to note that the characteristics of the Vlasov equation (3) correspond to the single-particle equations of motion in the applied field plus self-generated fields. For example, the coefficient of $\partial/\partial x$ is $dx/ds = x'$, the coefficient of $\partial/\partial x'$ is $dx'/ds = -\kappa_x(s)x - \partial\psi/\partial x$, etc. Moreover, the laboratory-frame Hamiltonian $\hat{H}$ for transverse single-particle motion consistent with Eqs. (3) and (4) is given (in dimensionless units) by

$$\hat{H}(x,y,x',y',s) = \frac{1}{2}(x'^2 + y'^2) + \frac{1}{2}[\kappa_x(s)x^2 + \kappa_y(s)y^2] + \psi(x,y,s). \tag{6}$$

For $\hat{H}$ specified by Eq. (6), Hamilton's equations, $d\mathbf{x}_\perp/ds = \partial\hat{H}/\partial\mathbf{x}'_\perp$ and $d\mathbf{x}'_\perp/ds = -\partial\hat{H}/\partial\mathbf{x}_\perp$, then give the equations of motion

$$\frac{d^2}{ds^2}x(s) + \kappa_x(s)x(s) = -\frac{\partial}{\partial x}\psi(x,y,s), \quad \frac{d^2}{ds^2}y(s) + \kappa_y(s)y(s) = -\frac{\partial}{\partial y}\psi(x,y,s), \tag{7}$$

for the transverse displacement, $\mathbf{x}_\perp(s) = x(s)\hat{\mathbf{e}}_x + y(s)\hat{\mathbf{e}}_y$, of an individual beam ion in the laboratory frame. In Sec. III, we will make use of Channell's third-order Hamiltonian averaging technique [34] to transform away the rapidly oscillating terms [35–38] in Eq. (6) and end up with a Hamiltonian $\mathcal{H}$ that depends only on slow variables (X, Y, X', Y').

In subsequent sections, we will consider two classes of periodic-focusing lattices. The first corresponds to an applied alternating-gradient quadrupole magnetic field [12],

$$\mathbf{B}_q^{\rm foc}(\mathbf{x}) = B_q'(s)\,(y\hat{\mathbf{e}}_x + x\hat{\mathbf{e}}_y)\,, \tag{8}$$

with coupling coefficient defined by

$$\kappa_x(s) = -\kappa_y(s) \equiv \kappa_q(s) = \frac{Z_b e B_q'(s)}{\gamma_b m_b \beta_b c^2}\,, \tag{9}$$

where $B_q'(s) \equiv (\partial B_x^q/\partial y)_{(0,0)} = (\partial B_y^q/\partial x)_{(0,0)}$. The second corresponds to a periodic-focusing solenoidal magnetic field [12,21],

$$\mathbf{B}_{\rm sol}^{\rm foc}(\mathbf{x}) = B_z(s)\hat{\mathbf{e}}_z - \frac{1}{2}B_z'(s)\,(x\hat{\mathbf{e}}_x + y\hat{\mathbf{e}}_y)\,, \tag{10}$$

with coupling coefficient defined by

$$\kappa_x(s) = \kappa_y(s) \equiv \kappa_s(s) = \left[\frac{Z_b e B_z(s)}{2\gamma_b m_b \beta_b c^2}\right]^2, \tag{11}$$

where $B_z'(s) \equiv (\partial B_z/\partial s)_{(0,0)}$. An important distinction between the two cases is evident. For a periodic quadrupole lattice, the average of $\kappa_q(s)$ over one lattice period S is zero, $\int_0^S ds\,\kappa_q(s) = 0$, and the periodic solutions to Eqs. (3) and (4) typically correspond to *elliptical* cross-section beams with oscillating (as a function of s) major and minor transverse dimensions, $a(s)$ and $b(s)$. On the other hand, for a periodic-focusing solenoidal field, the average of $\kappa_s(s)$ over one lattice period S is nonzero, $\int_0^S ds\,\kappa_s(s) = S\bar{\kappa}_s \neq 0$, and periodic solutions to Eqs. (3) and (4) typically correspond to *circular* cross-section beams with oscillating root-mean-square (rms) beam radius, $r_b(s)$. Furthermore, for the case of a solenoidal focusing field [Eq. (11)], the nonlinear Vlasov-Maxwell equations (3) and (4) are valid in a frame of reference rotating about the beam axis at the Larmor frequency [21], $\Omega_L(s) = -\omega_{cb}(s)/2 = -Z_b e B_z(s)/2\gamma_b m_b c$.

Following the third-order canonical transformation in Sec. III to the new Hamiltonian $\mathcal{H}$ in the slow variables (X, Y, X', Y'), in Secs. IV and V we examine the nonlinear Vlasov-Maxwell equations in the transformed variables and utilize the *back-transformation* to laboratory-frame variables (x, y, x', y'). In this regard, for specific choices of *equilibrium* distribution function $F_b^0(\mathcal{H}^0)$ with $\partial/\partial s = 0$ in the transformed variables, it is important to determine key physical properties of the (periodically focused) ion beam distribution function $f_b(x, y, x', y', s)$ in the laboratory frame. For future reference, in laboratory-frame variables, we denote the statistical average of a phase function $\chi(x, y, x', y', s)$ by

$$\langle\chi\rangle(s) = \frac{1}{N_b}\int dx\,dy\,dx'\,dy'\,\chi f_b\,, \tag{12}$$

where $N_b = \int dx\,dy\,dx'\,dy'\,f_b = $ const is the number of beam ions per unit axial length. One key property of the beam distribution function $f_b(x, y, x', y', s)$ is the density profile defined by

$$n_b(x, y, s) = \int dx'\,dy'\,f_b(x, y, x', y', s)\,. \tag{13}$$

Other important properties include the rms beam radius, $r_b(s)$, the rms x and y dimensions of the beam, $a(s)$ and $b(s)$, the unnormalized total transverse beam emittance, $\epsilon(s)$, and the unnormalized x- and y-transverse beam emittances, $\epsilon_x(s)$ and $\epsilon_y(s)$. These quantities are defined by

$$\begin{aligned}
&r_b^2(s) = \langle x^2 + y^2\rangle\,,\\
&a^2(s) = \langle x^2\rangle, \qquad b^2(s) = \langle y^2\rangle\,,\\
&\epsilon^2(s) = 4[\langle x'^2 + y'^2\rangle\langle x^2 + y^2\rangle - \langle xx' + yy'\rangle^2]\,,\\
&\epsilon_x^2(s) = 4[\langle x'^2\rangle\langle x^2\rangle - \langle xx'\rangle^2]\,,\\
&\epsilon_y^2(s) = 4[\langle y'^2\rangle\langle y^2\rangle - \langle yy'\rangle^2]\,,
\end{aligned} \tag{14}$$

where the statistical averages, $\langle\chi\rangle$, are defined according to Eq. (12).

III. CANONICAL TRANSFORMATION OF HAMILTONIAN AND PARTICLE COORDINATES TO SLOW VARIABLES

In this section, we make use of Channell's third-order Hamiltonian averaging technique [34] to transform from laboratory-frame variables (x, y, x', y') to the slow variables (X, Y, X', Y'), with a new Hamiltonian $\mathcal{H}(X, Y, X', Y', s)$. The formalism employs a canonical transformation given by an expanded generating function [34] to transform away the rapidly oscillating terms [35–38]. We formally express the laboratory-frame Hamiltonian $H(x, y, x', y', s)$ as

$$\begin{aligned}
H(x, y, x', y', s) &= \epsilon\hat{H}(x, y, x', y', s)\\
&= \epsilon\Big[\frac{1}{2}(x'^2 + y'^2) + V(x, y, s)\\
&\qquad + \psi(x, y, s)\Big]\,,
\end{aligned} \tag{15}$$

where $\hat{H}$ is defined in Eq. (6), and ϵ is a small dimensionless parameter. In Eq. (15), the applied focusing potential $V(x, y, s)$ is expressed as

$$V(x, y, s) = U(x, y) + \tilde{V}(x, y, s)\,, \tag{16}$$

where $U(x, y)$ is the steady (s-independent) contribution, and $\tilde{V}(x, y, s)$ is the rapidly oscillating part. For future reference, from Eqs. (6), (9), and (11) we express

$$\begin{aligned}
U(x, y) &= \frac{1}{2}[\bar{\kappa}_x x^2 + \bar{\kappa}_y y^2]\,,\\
\tilde{V}(x, y, s) &= \frac{1}{2}[\tilde{\kappa}_x(s)x^2 + \tilde{\kappa}_y(s)y^2]\,,
\end{aligned} \tag{17}$$

where the oscillating focusing coefficients are defined by $\tilde{\kappa}_x(s) = \kappa_x(s) - \bar{\kappa}_x$ and $\tilde{\kappa}_y(s) = \kappa_y(s) - \bar{\kappa}_y$, and the average focusing coefficients are defined by $\bar{\kappa}_x = S^{-1}\int_0^S ds\,\kappa_x(s)$ and $\bar{\kappa}_y = S^{-1}\int_0^S ds\,\kappa_y(s)$. For an alternating-gradient quadrupole field with $\int_0^S ds\,\kappa_q(s) = 0$ [Eq. (9)], it follows that

$$\begin{aligned} \bar{\kappa}_x &= -\bar{\kappa}_y = 0\,, \\ \tilde{\kappa}_x(s) &= -\tilde{\kappa}_y(s) \equiv \kappa_q(s)\,, \end{aligned} \tag{18}$$

and therefore $U_q(x,y) = 0$. On the other hand, for a periodic-focusing solenoidal field [Eq. (11)] with $\bar{\kappa}_s = S^{-1}\int_0^S ds\,\kappa_s(s) \neq 0$, it follows that

$$\begin{aligned} \bar{\kappa}_x &= \bar{\kappa}_y \equiv \bar{\kappa}_s \neq 0\,, \\ \tilde{\kappa}_x(s) &= \tilde{\kappa}_y(s) \equiv \tilde{\kappa}_s(s) = \kappa_s(s) - \bar{\kappa}_s\,, \end{aligned} \tag{19}$$

and therefore $U_{\rm sol}(x,y)$ is generally nonzero.

A. Canonical transformation

We introduce a near-identity canonical transformation where the expanded generation function [34] $S(x,y,X',Y',s)$ is defined by

$$S(x,y,X',Y',s) = xX' + yY' + \sum_{n=1}^{\infty}\epsilon^n S_n(x,y,X',Y',s)\,. \tag{20}$$

Here, (x,y,x',y') are the laboratory-frame variables, and (X,Y,X',Y') are the transformed variables. The transformed Hamiltonian $\mathcal{H}(X,Y,X',Y',s)$ in the new variables is given by

$$\mathcal{H}(X,Y,X',Y',s) = H(x,y,x',y',s) + \frac{\partial}{\partial s}S(x,y,X',Y',s)\,, \tag{21}$$

or equivalently, expressing $\mathcal{H} = \sum_{n=1}^{\infty}\epsilon^n \times \mathcal{H}_n(X,Y,X',Y',s)$ and making use of Eq. (15), Eq. (21) becomes

$$\sum_{n=1}^{\infty}\epsilon^n\mathcal{H}_n(X,Y,X',Y',s) = \epsilon\left[\frac{1}{2}(x'^2 + y'^2) + V(x,y,s) + \psi(x,y,s)\right] + \sum_{n=1}^{\infty}\epsilon^n\frac{\partial}{\partial s}S_n(x,y,X',Y',s)\,. \tag{22}$$

To determine the transformed Hamiltonian $\mathcal{H}(X,Y,X',Y',s)$, note that the variables (x,y,x',y') occurring on the right-hand sides of Eqs. (21) and (22) have to be expressed in terms of (X,Y,X',Y',s), i.e., $x = x(X,Y,X',Y',s)$, $x' = x'(X,Y,X',Y',s)$, etc. In this regard, the coordinate transformation generated by Eq. (20) is given by

$$\begin{aligned} X &= \frac{\partial S}{\partial X'} = x + \sum_{n=1}^{\infty}\epsilon^n\frac{\partial}{\partial X'}S_n(x,y,X',Y',s)\,, \\ Y &= \frac{\partial S}{\partial Y'} = y + \sum_{n=1}^{\infty}\epsilon^n\frac{\partial}{\partial Y'}S_n(x,y,X',Y',s)\,, \end{aligned} \tag{23}$$

and

$$\begin{aligned} x' &= \frac{\partial S}{\partial x} = X' + \sum_{n=1}^{\infty}\epsilon^n\frac{\partial}{\partial x}S_n(x,y,X',Y',s)\,, \\ y' &= \frac{\partial S}{\partial y} = Y' + \sum_{n=1}^{\infty}\epsilon^n\frac{\partial}{\partial y}S_n(x,y,X',Y',s)\,. \end{aligned} \tag{24}$$

Or, solving Eq. (23) iteratively for $x(X,Y,X',Y',s)$ and $y(X,Y,X',Y',s)$ gives

$$\begin{aligned} x &= X - \sum_{n=1}^{\infty}\epsilon^n\frac{\partial}{\partial X'}S_n(x,y,X',Y',s) \\ &= X + \sum_{n=1}^{\infty}\epsilon^n x_n(X,Y,X',Y',s)\,, \\ y &= Y - \sum_{n=1}^{\infty}\epsilon^n\frac{\partial}{\partial Y'}S_n(x,y,X',Y',s) \\ &= Y + \sum_{n=1}^{\infty}\epsilon^n y_n(X,Y,X',Y',s)\,, \end{aligned} \tag{25}$$

where

$$\begin{aligned} x_1(X,Y,X',Y',s) &= -\frac{\partial}{\partial X'}S_1(X,Y,X',Y',s)\,, \\ y_1(X,Y,X',Y',s) &= -\frac{\partial}{\partial Y'}S_1(X,Y,X',Y',s)\,, \end{aligned} \tag{26}$$

to leading order, etc. Similarly, solving Eq. (24) iteratively for $x'(X,Y,X',Y',s)$ and $y'(X,Y,X',Y',s)$ gives

$$\begin{aligned} x' &= X' + \sum_{n=1}^{\infty}\epsilon^n x'_n(X,Y,X',Y',s)\,, \\ y' &= Y' + \sum_{n=1}^{\infty}\epsilon^n y'_n(X,Y,X',Y',s)\,. \end{aligned} \tag{27}$$

where

$$\begin{aligned} x'_1(X,Y,X',Y',s) &= \frac{\partial}{\partial X}S_1(X,Y,X',Y',s)\,, \\ y'_1(X,Y,X',Y',s) &= \frac{\partial}{\partial Y}S_1(X,Y,X',Y',s)\,, \end{aligned} \tag{28}$$

to leading order, etc.

We now make use of Eqs. (25) and (27) to expand the Hamiltonian $H = \epsilon\hat{H}$ defined in Eq. (15). For example, making use of $x = X + \epsilon x_1 + \epsilon^2 x_2 + \cdots$ and $y = Y + \epsilon y_1 + \epsilon^2 y_2 + \cdots$, it is readily shown from Eqs. (16) and (17) that the applied focusing potential can be expressed as

$$\begin{aligned} V(x,y,s) = U(X,Y) &+ \tilde{V}_0(X,Y,s) \\ &+ \epsilon\tilde{V}_1(X,Y,X',Y',s) \\ &+ \epsilon^2\tilde{V}_2(X,Y,X',Y',s) + \cdots\,, \end{aligned} \tag{29}$$

correct to order ϵ^2. Here, the steady potential $U(X,Y)$ and the oscillating components, $\tilde{V}_j(X,Y,X',Y',s)$, $j=0,1,2$, are defined by

$$\begin{aligned} U(X,Y) &= \frac{1}{2}[\bar{\kappa}_x X^2 + \bar{\kappa}_y Y^2], \\ \tilde{V}_0(X,Y,s) &= \frac{1}{2}[\tilde{\kappa}_x(s)X^2 + \tilde{\kappa}_y(s)Y^2], \\ \tilde{V}_1(X,Y,X',Y',s) &= [\tilde{\kappa}_x(s) + \bar{\kappa}_x]x_1 X + [\tilde{\kappa}_y(s) + \bar{\kappa}_y]y_1 Y, \\ \tilde{V}_2(X,Y,X',Y',s) &= [\tilde{\kappa}_x(s) + \bar{\kappa}_x]\left(x_2 X + \frac{1}{2}x_1^2\right) + [\tilde{\kappa}_y(s) + \bar{\kappa}_y]\left(y_2 Y + \frac{1}{2}y_1^2\right). \end{aligned} \tag{30}$$

In Eq. (30), the oscillatory orbit perturbations, $x_1(X,Y,X',Y',s)$, $x_2(X,Y,X',Y',s)$, etc., are yet to be determined from Eq. (25). Similarly, we Taylor expand the self-field potential $\psi(x,y,s) = \psi(X + \epsilon x_1 + \epsilon^2 x_2 + \cdots, Y + \epsilon y_1 + \epsilon^2 y_2 + \cdots, s)$ occurring in the definition of H in Eq. (15). This readily gives

$$\psi(x,y,s) = \psi(X,Y,s) + \epsilon\tilde{\psi}_1(X,Y,X',Y',s) + \epsilon^2\tilde{\psi}_2(X,Y,X',Y',s) + \cdots. \tag{31}$$

Here, $\psi(X,Y,s)$ is the *slowly varying* self-field potential, and the oscillatory components, $\tilde{\psi}_1(X,Y,X',Y',s)$ and $\tilde{\psi}_2(X,Y,X',Y',s)$, are defined by

$$\begin{aligned} \tilde{\psi}_1(X,Y,X',Y',s) &= \left(x_1\frac{\partial}{\partial X} + y_1\frac{\partial}{\partial Y}\right)\psi(X,Y,s), \\ \tilde{\psi}_2(X,Y,X',Y',s) &= \left(x_2\frac{\partial}{\partial X} + y_2\frac{\partial}{\partial Y} + \frac{1}{2}x_1^2\frac{\partial^2}{\partial X^2} + \frac{1}{2}y_1^2\frac{\partial^2}{\partial Y^2} + x_1 y_1\frac{\partial^2}{\partial X\partial Y}\right)\psi(X,Y,s). \end{aligned} \tag{32}$$

Finally, making use of $x' = X' + \epsilon x_1' + \epsilon^2 x_2' + \cdots$ and $y' = Y' + \epsilon y_1' + \epsilon^2 y_2' + \cdots$ in the kinetic energy contribution, $(1/2)(x'^2 + y'^2)$, to the definition of $H = \epsilon\hat{H}$ in Eq. (15), we obtain

$$\frac{1}{2}(x'^2 + y'^2) = \frac{1}{2}(X'^2 + Y'^2) + \epsilon(x_1'X' + y_1'Y') + \epsilon^2\left[(x_2'X' + y_2'Y') + \frac{1}{2}(x_1'^2 + y_1'^2)\right] + \cdots. \tag{33}$$

In Eq. (33), the oscillatory velocity perturbations, $x_1'(X,Y,X',Y',s)$, $x_2'(X,Y,X',Y',s)$, etc., are yet to be determined from Eqs. (24) and (27).

We now collect together the results in Eqs. (29)–(33) and substitute them into the expression for the transformed Hamiltonian $\mathcal{H}(X,Y,X',Y',s) = \sum\epsilon^n\mathcal{H}_n(X,Y,X',Y',s)$ in Eq. (22). This readily gives

$$\begin{aligned} \sum_{n=1}^{\infty}\epsilon^n\mathcal{H}_n(X,Y,X',Y',s) = \epsilon\Big\{&\frac{1}{2}(X'^2 + Y'^2) + U(X,Y) + \psi(X,Y,s) + \tilde{V}_0(X,Y,s) \\ &+ \epsilon[(x_1'X' + y_1'Y') + \tilde{V}_1(X,Y,X',Y',s) + \tilde{\psi}_1(X,Y,X',Y',s)] \\ &+ \epsilon^2\Big[(x_2'X' + y_2'Y') + \frac{1}{2}(x_1'^2 + y_1'^2) + \tilde{V}_2(X,Y,X',Y',s) \\ &\qquad + \tilde{\psi}_2(X,Y,X',Y',s)\Big] + \cdots\Big\} \\ &+ \sum_{n=1}^{\infty}\epsilon^n\frac{\partial}{\partial s}S_n\big(x(X,Y,X',Y',s), y(X,Y,X',Y',s), X', Y', s\big), \end{aligned} \tag{34}$$

where the oscillatory potentials $\tilde{V}_0$, $\tilde{V}_1$, $\tilde{V}_2$, $\tilde{\psi}_1$, and $\tilde{\psi}_2$ are defined in Eqs. (30) and (31). The main objective of the present analysis is to transform to new coordinates (X,Y,X',Y') such that the transformed Hamiltonian $\mathcal{H}(X,Y,X',Y',s) = \sum_{n=1}^{\infty}\epsilon^n\mathcal{H}_n(X,Y,X',Y',s)$ is *slowly varying.* Thus far, the generating function $S(x,y,X',Y',s) = \sum_{n=1}^{\infty}\epsilon^n S_n(x,y,X',Y',s)$ has been arbitrary and unspecified. We now make use of this freedom to choose $\{S_n\}$ in such a way that the transformed Hamiltonian $\mathcal{H}(X,Y,X',Y',s)$ is slowly varying correct to third order in the expansion parameter ϵ. The analysis will involve s integrations over the periodic lattice functions $\tilde{\kappa}_x(s+S) = \tilde{\kappa}_x(s)$ and $\tilde{\kappa}_y(s+S) = \tilde{\kappa}_y(s)$. For future reference, it is convenient to introduce the definitions of several key quantities that occur in the subsequent analysis. The definitions are

$$
\begin{aligned}
\alpha_x(s) &= \int_0^s ds\, \tilde{\kappa}_x(s), & \alpha_y(s) &= \int_0^s ds\, \tilde{\kappa}_y(s)\,, \\
\langle\alpha_x\rangle &= \frac{1}{S}\int_0^S ds\, \alpha_x(s), & \langle\alpha_y\rangle &= \frac{1}{S}\int_0^S ds\, \alpha_y(s)\,, \\
\beta_x(s) &= \int_0^s ds[\alpha_x(s) - \langle\alpha_x\rangle], & \beta_y(s) &= \int_0^s ds[\alpha_y(s) - \langle\alpha_y\rangle]\,, \\
\langle\beta_x\rangle &= \frac{1}{S}\int_0^S ds\, \beta_x(s), & \langle\beta_y\rangle &= \frac{1}{S}\int_0^S ds\, \beta_y(s)\,, \\
\delta_x(s) &= \alpha_x^2(s) - 2\tilde{\kappa}_x(s)\beta_x(s), & \delta_y(s) &= \alpha_y^2(s) - 2\tilde{\kappa}_y(s)\beta_y(s)\,, \\
\langle\delta_x\rangle &= \frac{1}{S}\int_0^S ds\, \delta_x(s), & \langle\delta_y\rangle &= \frac{1}{S}\int_0^S ds\, \delta_y(s)\,.
\end{aligned}
\tag{35}
$$

We now solve Eq. (34) order by order, beginning with order ϵ.

1. Canonical transformation to order ϵ

Setting the coefficient of the terms of order ϵ equal to zero in Eq. (34) gives for the first-order transformed Hamiltonian $\mathcal{H}_1(X, Y, X', Y', s)$

$$
\begin{aligned}
\mathcal{H}_1 = \frac{1}{2}(X'^2 + Y'^2) + U(X,Y) + \psi(X,Y,s) \\
+ \tilde{V}_0(X,Y,s) + \frac{\partial}{\partial s} S_1\,,
\end{aligned}
\tag{36}
$$

where $U(X,Y)$ is the steady confining potential defined in Eq. (30), $\psi(X,Y,s)$ is the slowly varying self-field potential, and the lowest-order oscillatory confining potential $\tilde{V}_0(X,Y,s)$ is defined in Eq. (30). To assure that $\mathcal{H}_1$ is slowly varying, we choose the first-order generating function S_1 in Eq. (36) so that the final two terms on the right-hand side of Eq. (36) exactly cancel. Integrating from $s = 0$, this readily gives

$$
\begin{aligned}
S_1(X,Y,s) &= -\int_0^s ds\, \tilde{V}_0(X,Y,s) \\
&= -\frac{1}{2}[\alpha_x(s)X^2 + \alpha_y(s)Y^2],
\end{aligned}
\tag{37}
$$

where $\alpha_x(s)$ and $\alpha_y(s)$ are defined in Eq. (35). Because $\partial S_1/\partial s = -\tilde{V}_0(X,Y,s)$, the expression for $\mathcal{H}_1(X,Y,X',Y',s)$ in Eq. (36) reduces to

$$
\mathcal{H}_1 = \frac{1}{2}(X'^2 + Y'^2) + U(X,Y) + \psi(X,Y,s)\,, \tag{38}
$$

which is slowly varying because of the choice of S_1 in Eq. (37). From Eqs. (26), (28), and (37), it also follows that the first-order transverse displacement coordinates (x_1, y_1) and velocity coordinates (x_1', y_1') are given by

$$
\begin{aligned}
x_1 &= -\frac{\partial}{\partial X'} S_1 = 0\,, \\
y_1 &= -\frac{\partial}{\partial Y'} S_1 = 0\,,
\end{aligned}
\tag{39}
$$

and

$$
\begin{aligned}
x_1' &= \frac{\partial S_1}{\partial X} = -\alpha_x(s)X\,, \\
y_1' &= \frac{\partial S_1}{\partial Y} = -\alpha_y(s)Y\,.
\end{aligned}
\tag{40}
$$

Eqs. (39) and (40) lead to several simplifications in the subsequent analysis. In particular, from Eqs. (30), (32), (39), and (40), it follows that the first- and second-order contributions to the oscillatory focusing-field potential are given by

$$
\begin{aligned}
\tilde{V}_1(X,Y,X',Y',s) &= 0\,, \\
\tilde{V}_2(X,Y,X',Y',s) &= [\tilde{\kappa}_x(s) + \bar{\kappa}_x]x_2 X \\
&\quad + [\tilde{\kappa}_y(s) + \bar{\kappa}_y]y_2 Y\,,
\end{aligned}
\tag{41}
$$

and the first- and second-order contributions to the oscillatory self-field potential are given by

$$
\begin{aligned}
\tilde{\psi}_1(X,Y,X',Y',s) &= 0\,, \\
\tilde{\psi}_2(X,Y,X',Y',s) &= \left(x_2\frac{\partial}{\partial X} + y_2\frac{\partial}{\partial Y}\right)\psi(X,Y,s)\,.
\end{aligned}
\tag{42}
$$

In Eqs. (41) and (42), the second-order perturbed orbits $x_2(X,Y,X',Y',s)$ and $y_2(X,Y,X',Y',s)$ are yet to be determined.

2. Canonical transformation to order ϵ^2

We now make use of $\tilde{V}_1 = 0 = \tilde{\psi}_1$ and $x_1 = 0 = y_1$ and set the coefficient of ϵ^2 equal to zero in Eq. (34). This gives for the second-order transformed Hamiltonian $\mathcal{H}_2(X,Y,X',Y',s)$

$$
\begin{aligned}
\mathcal{H}_2 &= x_1'X' + y_1'Y' + \frac{\partial}{\partial s} S_2 \\
&= -\alpha_x(s)XX' - \alpha_y(s)YY' + \frac{\partial}{\partial s} S_2\,,
\end{aligned}
\tag{43}
$$

where (x_1', y_1') is defined in Eq. (40), and the coefficients $\alpha_x(s)$ and $\alpha_y(s)$ are defined in Eq. (35). We rewrite Eq. (43) in the equivalent form

$$\mathcal{H}_2 = -\langle\alpha_x\rangle XX' - \langle\alpha_y\rangle YY' - [\alpha_x(s) - \langle\alpha_x\rangle]XX' - [\alpha_y(s) - \langle\alpha_y\rangle]YY' + \frac{\partial}{\partial s}S_2\,, \tag{44}$$

where $\langle\alpha_x\rangle \equiv S^{-1}\int_0^S ds\,\alpha_x(s)$ and $\langle\alpha_y\rangle \equiv S^{-1}\int_0^S ds\,\alpha_y(s)$. To assure that $\mathcal{H}_2(X, Y, X', Y', s)$ is slowly varying, we choose the second-order generating function S_2 in Eq. (44) such that

$$S_2 = XX'\int_0^s ds[\alpha_x(s) - \langle\alpha_x\rangle] + YY'\int_0^s ds[\alpha_y(s) - \langle\alpha_y\rangle] = \beta_x(s)XX' + \beta_y(s)YY', \tag{45}$$

where the oscillatory coefficients $\beta_x(s)$ and $\beta_y(s)$ are defined in Eq. (35). Substituting Eq. (45) into Eq. (44) then gives for the second-order transformed Hamiltonian $\mathcal{H}_2(X, Y, X', Y', s)$

$$\mathcal{H}_2 = -\langle\alpha_x\rangle XX' - \langle\alpha_y\rangle YY', \tag{46}$$

where the coefficients $\langle\alpha_x\rangle$ and $\langle\alpha_y\rangle$ are constants (independent of s). Furthermore, from Eqs. (24), (25), (27), and (45), the second-order transverse displacement coordinates (x_2, y_2) and velocity coordinates (x_2', y_2') are given by

$$\begin{aligned} x_2 &= -\frac{\partial}{\partial X'}S_2 = -\beta_x(s)X\,, \\ y_2 &= -\frac{\partial}{\partial Y'}S_2 = -\beta_y(s)Y\,, \end{aligned} \tag{47}$$

and

$$\begin{aligned} x_2' &= \frac{\partial}{\partial X}S_2 = \beta_x(s)X', \\ y_2' &= \frac{\partial}{\partial Y}S_2 = \beta_y(s)Y'. \end{aligned} \tag{48}$$

As a general remark, from the definitions of the oscillatory coefficients, $\beta_x(s)$ and $\beta_y(s)$, in Eq. (35), we note that

$$\begin{aligned} \beta_x(s + S) &= \beta_x(s)\,, \\ \beta_y(s + S) &= \beta_y(s)\,, \end{aligned} \tag{49}$$

and that $\beta_x(s = 0) = 0 = \beta_x(s = S)$ and $\beta_y(s = 0) = 0 = \beta_y(s = S)$.

3. Canonical transformation to order ϵ^3

Returning to the expression for the transformed Hamiltonian $\mathcal{H}$ in Eq. (34), we set the coefficient of ϵ^3 equal to zero and make use of the definitions of $\tilde{V}_2(X, Y, X', Y', s)$ and $\tilde{\psi}_2(X, Y, X', Y', s)$ in Eqs. (41) and (42). This gives, for the third-order Hamiltonian $\mathcal{H}_3(X, Y, X', Y', s)$,

$$\begin{aligned} \mathcal{H}_3 = {}& x_2'X' + y_2'Y' + \frac{1}{2}(x_1'^2 + y_1'^2) \\ & + [\tilde{\kappa}_x(s) + \bar{\kappa}_x]x_2X + [\tilde{\kappa}_y(s) + \bar{\kappa}_y]y_2Y \\ & + x_2\frac{\partial\psi}{\partial X} + y_2\frac{\partial\psi}{\partial Y} + \frac{\partial S_3}{\partial s}\,. \end{aligned} \tag{50}$$

Making use of the expressions for (x_1', y_1'), (x_2, y_2), and (x_2', y_2') in Eqs. (40), (47), and (48), it is straightforward to show that Eq. (50) can be expressed as

$$\begin{aligned} \mathcal{H}_3 = {}& \beta_x(s)\left[X'^2 - \bar{\kappa}_xX^2 - X\frac{\partial\psi}{\partial X}\right] + \beta_y(s)\left[Y'^2 - \bar{\kappa}_yY^2 - Y\frac{\partial\psi}{\partial Y}\right] + \frac{1}{2}[\alpha_x^2(s) - 2\tilde{\kappa}_x(s)\beta_x(s)]X^2 \\ & + \frac{1}{2}[\alpha_y^2(s) - 2\tilde{\kappa}_y(s)\beta_y(s)]Y^2 + \frac{\partial S_3}{\partial s}\,, \end{aligned} \tag{51}$$

where the s-dependent factors $\beta_x(s)$, $\beta_y(s)$, $\alpha_x(s)$, and $\alpha_y(s)$ are defined in Eq. (35) in terms of the periodic lattice functions $\tilde{\kappa}_x(s + S) = \tilde{\kappa}_x(s)$ and $\tilde{\kappa}_y(s + S) = \tilde{\kappa}_y(s)$. For the applications of interest here, not only are the averages $\int_0^S ds\,\tilde{\kappa}_x(s) = 0$ and $\int_0^S ds\,\tilde{\kappa}_y(s) = 0$, but the lattice functions $\tilde{\kappa}_x(s)$ and $\tilde{\kappa}_y(s)$ are assumed to have odd half-period symmetry (see examples in Fig. 1) with

$$\begin{aligned} \tilde{\kappa}_x(s - S/2) &= -\tilde{\kappa}_x[-(s - S/2)]\,, \\ \tilde{\kappa}_y(s - S/2) &= -\tilde{\kappa}_y[-(s - S/2)]\,. \end{aligned} \tag{52}$$

Some straightforward integration by parts that makes use of the definitions in Eq. (35) shows that the averages $\langle\beta_x\rangle$ and $\langle\beta_y\rangle$ can be expressed as

$$\begin{aligned} \langle\beta_x\rangle &= \frac{1}{2S}\int_0^S ds(s^2 - sS)\tilde{\kappa}_x(s) = \frac{1}{2S}\int_0^S ds\left(s - \frac{S}{2}\right)^2\tilde{\kappa}_x(s)\,, \\ \langle\beta_y\rangle &= \frac{1}{2S}\int_0^S ds(s^2 - sS)\tilde{\kappa}_y(s) = \frac{1}{2S}\int_0^S ds\left(s - \frac{S}{2}\right)^2\tilde{\kappa}_y(s)\,, \end{aligned} \tag{53}$$

and the averages $\langle\alpha_x\rangle$ and $\langle\alpha_y\rangle$ can be expressed as

$$\langle \alpha_x \rangle = -\frac{1}{S}\int_0^S ds\, s\tilde{\kappa}_x(s) = -\frac{1}{S}\int_0^S ds\left(s - \frac{S}{2}\right)\tilde{\kappa}_x(s)\,,$$
$$\langle \alpha_y \rangle = -\frac{1}{S}\int_0^S ds\, s\tilde{\kappa}_y(s) = -\frac{1}{S}\int_0^S ds\left(s - \frac{S}{2}\right)\tilde{\kappa}_y(s)\,. \tag{54}$$

It therefore follows from Eqs. (52)–(54) that

$$\langle \beta_x \rangle = 0 = \langle \beta_y \rangle\,, \tag{55}$$

whereas $\langle \alpha_x \rangle$ and $\langle \alpha_y \rangle$ are generally nonzero.

We now return to the third-order Hamiltonian in Eq. (51) and choose the generating function S_3 to exactly cancel all rapidly oscillating terms on the right-hand side of Eq. (51). Because $\langle \beta_x \rangle = 0 = \langle \beta_y \rangle$, we pick

$$S_3 = -\int_0^s ds\, \beta_x(s)\left[X'^2 - \bar{\kappa}_x X^2 - X\frac{\partial \psi}{\partial X}\right] - \int_0^s ds\, \beta_y(s)\left[Y'^2 - \bar{\kappa}_y Y^2 - Y\frac{\partial \psi}{\partial Y}\right]$$
$$- \frac{1}{2}\left(\int_0^s ds[\delta_x(s) - \langle \delta_x \rangle]\right)X^2 - \frac{1}{2}\left(\int_0^s ds[\delta_y(s) - \langle \delta_y \rangle]\right)Y^2. \tag{56}$$

Here, $\delta_x(s) \equiv \alpha_x^2(s) - 2\tilde{\kappa}_x(s)\beta_x(s)$ and $\delta_y(s) \equiv \alpha_y^2(s) - 2\tilde{\kappa}_y(s)\beta_y(s)$, and $\langle \delta_x \rangle \equiv S^{-1}\int_0^S ds\, \delta_x(s)$ and $\langle \delta_y \rangle \equiv S^{-1}\int_0^S ds\, \delta_y(s)$. Substituting Eq. (56) into Eq. (51) then gives for the slowly varying third-order Hamiltonian $\mathcal{H}_3(X, Y, X', Y', s)$

$$\mathcal{H}_3 = \frac{1}{2}\langle \delta_x \rangle X^2 + \frac{1}{2}\langle \delta_y \rangle Y^2. \tag{57}$$

For future reference, we further simplify the expressions for $\langle \delta_x \rangle$ and $\langle \delta_y \rangle$. Making use of Eq. (35), $\tilde{\kappa}_x(s) = d\alpha_x/ds$ and $d\beta_x/ds = \alpha_x(s) - \langle \alpha_x \rangle$, gives

$$\langle \delta_x \rangle = \frac{1}{S}\int_0^S ds\left(\alpha_x^2 - 2\frac{d\alpha_x}{ds}\beta_x\right) = \frac{1}{S}\int_0^S ds\left[\alpha_x^2 - 2\frac{d}{ds}(\alpha_x\beta_x) + 2\alpha_x(\alpha_x - \langle \alpha_x \rangle)\right]. \tag{58}$$

Making use of the fact that $\beta_x(s)$ and $\beta_y(s)$ vanish at $s = 0$ and $s = S$, Eq. (58) readily gives the compact representations

$$\langle \delta_x \rangle = \frac{1}{S}\int_0^S ds[3\alpha_x^2(s) - 2\langle \alpha_x \rangle^2]\,,$$
$$\langle \delta_y \rangle = \frac{1}{S}\int_0^S ds[3\alpha_y^2(s) - 2\langle \alpha_y \rangle^2]\,. \tag{59}$$

Finally, making use of Eqs. (24), (25), (27), and (56), the third-order transverse displacement coordinates (x_3, y_3) and velocity coordinates (x_3', y_3') are given by

$$x_3 = -\frac{\partial S_3}{\partial X'} = 2\int_0^s ds\, \beta_x(s)X'\,,$$
$$y_3 = -\frac{\partial S_3}{\partial Y'} = 2\int_0^s ds\, \beta_y(s)Y'\,, \tag{60}$$

and

$$x_3' = \frac{\partial S_3}{\partial X} - x_2\frac{\partial^2 S_1}{\partial X^2} = \int_0^s ds\, \beta_x(s)\left[2\bar{\kappa}_x X + \frac{\partial}{\partial X}\left(X\frac{\partial \psi}{\partial X}\right)\right] + \int_0^s ds\, \beta_y(s)\left[\frac{\partial}{\partial X}\left(Y\frac{\partial \psi}{\partial Y}\right)\right]$$
$$- \left(\int_0^s ds[\delta_x(s) - \langle \delta_x \rangle]\right)X - \alpha_x(s)\beta_x(s)X\,,$$
$$y_3' = \frac{\partial S_3}{\partial Y} - y_2\frac{\partial^2 S_1}{\partial Y^2} = \int_0^s ds\, \beta_y(s)\left[2\bar{\kappa}_y Y + \frac{\partial}{\partial Y}\left(Y\frac{\partial \psi}{\partial Y}\right)\right] + \int_0^s ds\, \beta_x(s)\left[\frac{\partial}{\partial Y}\left(X\frac{\partial \psi}{\partial X}\right)\right]$$
$$- \left(\int_0^s ds[\delta_y(s) - \langle \delta_y \rangle]\right)Y - \alpha_y(s)\beta_y(s)Y\,. \tag{61}$$

Here, use has been made of the expressions for $S_1(X,Y,s)$ and (x_2,y_2) in Eqs. (37) and (47), and the $O(\epsilon^3)$ contributions to x_3' and y_3' from $\epsilon S_1(X,Y,s) = \epsilon S_1(x - \epsilon^2 x_2, y - \epsilon^2 y_2, s)$, have been included by Taylor expansion in Eq. (24).

B. Third-order transformed Hamiltonian and coordinate transformation

The averaging approach developed in Sec. III A represents a powerful formalism for determining the third-order slowly varying Hamiltonian $\mathcal{H}(X,Y,X',Y',s) = \epsilon\mathcal{H}_1 + \epsilon^2\mathcal{H}_2 + \epsilon^3\mathcal{H}_3 + \cdots$ and the corresponding coordinate transformations $x(X,Y,X',Y',s) = X + \epsilon x_1 + \epsilon^2 x_2 + \epsilon^3 x_3 + \cdots$, $x'(X,Y,X',Y',s) = X' + \epsilon x_1' + \epsilon^2 x_2' + \epsilon^3 x_3' + \cdots$, etc. From Eqs. (38), (46), and (57), we obtain, correct to third order in ϵ,

$$\begin{aligned}\mathcal{H}(X,Y,X',Y',s) = {}& \frac{1}{2}(X'^2 + Y'^2) + U(X,Y) \\ &+ \psi(X,Y,s) - [\langle\alpha_x\rangle XX' + \langle\alpha_y\rangle YY'] \\ &+ \frac{1}{2}\langle\delta_x\rangle X^2 + \frac{1}{2}\langle\delta_y\rangle Y^2, \end{aligned} \tag{62}$$

where $\langle\alpha_x\rangle$, $\langle\alpha_y\rangle$, $\langle\delta_x\rangle$, and $\langle\delta_y\rangle$ are defined in Eqs. (35) and (59), and we have set the expansion parameter $\epsilon = 1$. In Eq. (62), $U(X,Y)$ is the steady focusing potential defined by $U(X,Y) = (1/2)(\bar{\kappa}_x X^2 + \bar{\kappa}_y Y^2)$, and $\psi(X,Y,s)$ is the slowly varying self-field potential in the transformed variables. It is useful to introduce the average focusing coefficients κ_{fx} and κ_{fy} defined by

$$\begin{aligned}\kappa_{fx} &\equiv \frac{3}{S}\int_0^S ds[\alpha_x^2(s) - \langle\alpha_x\rangle^2] = \text{const}, \\ \kappa_{fy} &\equiv \frac{3}{S}\int_0^S ds[\alpha_y^2(s) - \langle\alpha_y\rangle^2] = \text{const}. \end{aligned} \tag{63}$$

Rearranging terms in Eq. (62), and making use of Eqs. (59) and (63), it follows that Eq. (62) can be expressed in the equivalent form

$$\begin{aligned}\mathcal{H}(X,Y,X',Y',s) = {}& \frac{1}{2}[(X' - \langle\alpha_x\rangle X)^2 + (Y' - \langle\alpha_y\rangle Y)^2] \\ &+ U(X,Y) + \frac{1}{2}(\kappa_{fx}X^2 + \kappa_{fy}Y^2) \\ &+ \psi(X,Y,s). \end{aligned} \tag{64}$$

For completeness, it should be pointed out that if we introduce the additional canonical transformation (known as a fiber transformation) to variables $(\tilde{X},\tilde{Y},\tilde{X}',\tilde{Y}')$ defined by [38]

$$\begin{aligned}\tilde{X} &= X, & \tilde{Y} &= Y, \\ \tilde{X}' &= X' - \langle\alpha_x\rangle X, & \tilde{Y}' &= Y' - \langle\alpha_y\rangle Y, \end{aligned} \tag{65}$$

then the transformed Hamiltonian in Eq. (64) can also be expressed as

$$\begin{aligned}\mathcal{H}(\tilde{X},\tilde{Y},\tilde{X}',\tilde{Y}',s) = {}& \frac{1}{2}(\tilde{X}'^2 + \tilde{Y}'^2) \\ &+ U(\tilde{X},\tilde{Y}) + \psi(\tilde{X},\tilde{Y},s) \\ &+ \frac{1}{2}(\kappa_{fx}\tilde{X}^2 + \kappa_{fy}\tilde{Y}^2). \end{aligned} \tag{66}$$

For future reference in Sec. IV, we now simplify the expression for the transformed Hamiltonian $\mathcal{H}$ defined in Eq. (64) for the two cases corresponding to: (a) the alternating-gradient quadrupole focusing field in Eqs. (9) and (18) and (b) the periodic-focusing solenoidal field in Eqs. (11) and (19).

1. Transformed Hamiltonian for an alternating-gradient quadrupole field

In this case, $\bar{\kappa}_x(s) = -\bar{\kappa}_y(s) = \kappa_q(s)$ and $\bar{\kappa}_x = -\bar{\kappa}_y = S^{-1}\int_0^S ds\,\kappa_q(s) = 0$, and it follows that

$$\begin{aligned}\alpha_x(s) &= -\alpha_y(s) = \alpha_q(s) \equiv \int_0^s ds\,\kappa_q(s), \\ \langle\alpha_x\rangle &= -\langle\alpha_y\rangle = \langle\alpha_q\rangle \equiv \frac{1}{S}\int_0^S ds\,\alpha_q(s), \\ \beta_x(s) &= -\beta_y(s) = \beta_q(s) \equiv \frac{1}{S}\int_0^s ds[\alpha_q(s) - \langle\alpha_q\rangle], \\ \langle\beta_x\rangle &= -\langle\beta_y\rangle = \langle\beta_q\rangle = 0, \\ \delta_x(s) &= \delta_y(s) = \delta_q(s) \equiv \alpha_q^2(s) - 2\kappa_q(s)\beta_q(s), \\ \langle\delta_x\rangle &= \langle\delta_y\rangle = \langle\delta_q\rangle \equiv \frac{1}{S}\int_0^S ds[3\alpha_q^2(s) - 2\langle\alpha_q\rangle^2], \\ \kappa_{fx} &= \kappa_{fy} = \kappa_{fq} \equiv \frac{3}{S}\int_0^S ds[\alpha_q^2(s) - \langle\alpha_q\rangle^2]. \end{aligned} \tag{67}$$

From Eqs. (64) and (67), for a periodic quadrupole lattice with $\kappa_q(s+S) = \kappa_q(s)$ and $S^{-1}\int_0^S ds\,\kappa_q(s) = 0$, it follows that the slowly varying Hamiltonian $\mathcal{H}_q(X,Y,X',Y',s)$ is given correct to third order in ϵ by the expression

$$\begin{aligned}\mathcal{H}_q(X,Y,X',Y',s) = {}& \frac{1}{2}[(X' - \langle\alpha_q\rangle X)^2 \\ &+ (Y' + \langle\alpha_q\rangle Y)^2] \\ &+ \frac{1}{2}\kappa_{fq}(X^2 + Y^2) + \psi(X,Y,s). \end{aligned} \tag{68}$$

Here, $\kappa_{fq} \equiv (3/S)\int_0^S ds[\alpha_q^2(s) - \langle\alpha_q\rangle^2]$ is the average quadrupole focusing coefficient, and use has been made of $U_q(X,Y) = (1/2)(\bar{\kappa}_x X^2 + \bar{\kappa}_y Y^2) = 0$ because $\int_0^S ds\,\kappa_q(s) = 0$.

For purposes of illustration, listed in Table I are the values of the lattice functions defined in Eq. (67) for the choice of a periodic-focusing quadrupole lattice with $\kappa_q(s) = \hat{\kappa}_q \sin(2\pi s/S)$, where $\hat{\kappa}_q = \text{const}$. Here, we have introduced the dimensionless amplitude defined by $\lambda_q \equiv \hat{\kappa}_q S^2/2\pi$ and the lattice wave number defined by

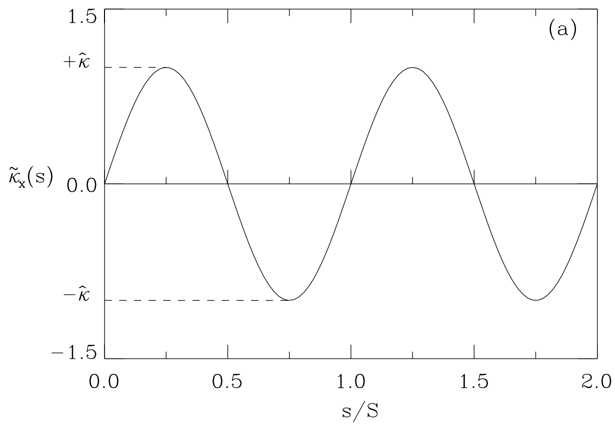

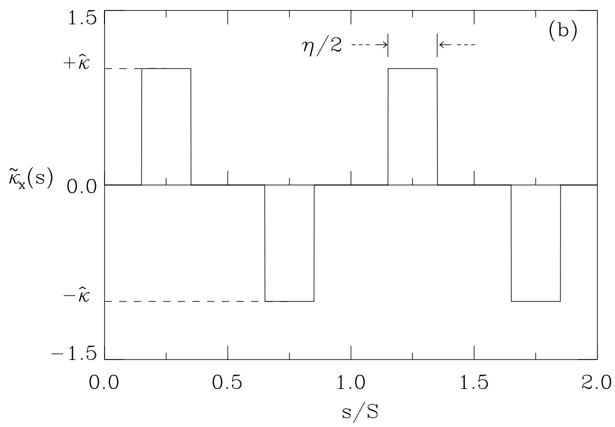

FIG. 1. Examples of periodic-focusing lattice functions with odd half-period symmetry [Eq. (52)] corresponding to (a) a sinusoidal lattice function, $\tilde{\kappa}_x(s) = \hat{\kappa}\sin(2\pi s/S)$, with $\hat{\kappa} =$ const, and (b) a periodic step-function lattice with amplitude $\hat{\kappa} =$ const and filling factor η.

$k_s = S/2\pi$. An identical set of values is obtained from Eq. (69) for a periodic-focusing solenoidal lattice with $\tilde{\kappa}_s(s) = \hat{\kappa}_s \sin(2\pi s/S)$.

2. Transformed Hamiltonian for a periodic-focusing solenoidal field

In this case, from Eqs. (11) and (19), $\tilde{\kappa}_s(s) = \kappa_s(s) - \bar{\kappa}_s$, where $\bar{\kappa}_s = S^{-1}\int_0^S ds\,\kappa_s(s) \neq 0$ and $S^{-1}\int_0^S ds \times \tilde{\kappa}_s(s) = 0$, and there is a high degree of symmetry about the beam axis because $\tilde{\kappa}_x(s) = \tilde{\kappa}_y(s) \equiv \tilde{\kappa}_s(s)$. In particular, from Eqs. (35), (59), and (63), we find

$$\begin{aligned}
\alpha_x(s) &= \alpha_y(s) = \alpha_s(x) \equiv \int_0^s ds\,\tilde{\kappa}_s(s)\,, \\
\langle\alpha_x\rangle &= \langle\alpha_y\rangle = \langle\alpha_s\rangle = \frac{1}{S}\int_0^S ds\,\alpha_s(s)\,, \\
\beta_x(s) &= \beta_y(s) = \beta_s(s) \equiv \frac{1}{S}\int_0^s ds[\alpha_s(s) - \langle\alpha_s\rangle]\,, \\
\langle\beta_x\rangle &= \langle\beta_y\rangle = \langle\beta_s\rangle = 0\,, \qquad (69) \\
\delta_x(s) &= \delta_y(s) = \delta_s(s) \equiv \alpha_s^2(s) - 2\tilde{\kappa}_s(s)\beta_s(s)\,, \\
\langle\delta_x\rangle &= \langle\delta_y\rangle = \langle\delta_s\rangle \equiv \frac{1}{S}\int_0^S ds[3\alpha_s^2(s) - 2\langle\alpha_s\rangle^2]\,, \\
\kappa_{fx} &= \kappa_{fy} = \kappa_{fs} \equiv \frac{3}{S}\int_0^S ds[\alpha_s^2(s) - \langle\alpha_s\rangle^2]\,.
\end{aligned}$$

From Eqs. (64) and (69), for a periodic-focusing solenoidal field with $\kappa_s(s+S) = \kappa_s(s)$ and $S^{-1}\int_0^S ds\,\kappa_s(s) = \bar{\kappa}_s \neq 0$, it follows that the slowly varying Hamiltonian $\mathcal{H}_s(X,Y,X',Y',s)$ is given correct to third order in ϵ by

$$\mathcal{H}_s(X,Y,X',Y',s) = \frac{1}{2}[(X' - \langle\alpha_s\rangle X)^2 + (Y' - \langle\alpha_s\rangle Y)^2] + \frac{1}{2}(\bar{\kappa}_s + \kappa_{fs})(X^2 + Y^2) + \psi(X,Y,s)\,. \qquad (70)$$

Here, use has been made of $U_s(X,Y) = (1/2)\bar{\kappa}_s(X^2 + Y^2)$, and $\kappa_{fs} \equiv (3/S)\int_0^S ds[\alpha_s^2(s) - \langle\alpha_s\rangle^2]$ is the average focusing coefficient associated with the oscillating lattice coefficient $\tilde{\kappa}_s(s+S) = \tilde{\kappa}_s(s)$.

To conclude Sec. III, we collect together the results for the coordinate transformations $x(X,Y,X',Y',s) = X + \epsilon x_1 + \epsilon^2 x_2 + \epsilon^3 x_3 + \cdots$, $x'(X,Y,X',Y',s) = X' + \epsilon x_1' + \epsilon^2 x_2' + \epsilon^3 x_3' + \cdots$, etc., obtained correct to order ϵ^3 from Eqs. (39), (40), (47), (48), (60), and (61). Again, we distinguish the two cases corresponding to (a) an alternating-gradient quadrupole field described by Eqs. (9) and (18) and (b) a periodic-focusing solenoidal field described by Eqs. (11) and (19), making use of the related symmetries in Eqs. (67) and (69).

TABLE I. Values of lattice functions defined in Eq. (67) for a periodic quadrupole lattice with $\kappa_q(s) = \hat{\kappa}_q \sin(2\pi s/S)$, with $\hat{\kappa}_q =$ const. Here, $\lambda_q \equiv \hat{\kappa}_q S^2/2\pi$ and $k_s \equiv 2\pi/S$.

Function	Value	Function	Value
$\alpha_q(s)$	$\frac{\lambda_q}{S}[1 - \cos(k_s s)]$	$\delta_q(s)$	$\frac{\lambda_q^2}{S^2}[2 + \sin^2(k_s s) - 2\cos(k_s s)]$
$\langle\alpha_q\rangle$	$\frac{\lambda_q}{S}$	$\langle\delta_q\rangle$	$\frac{5}{2}\frac{\lambda_q^2}{S^2}$
$\alpha_q(s) - \langle\alpha_q\rangle$	$-\frac{\lambda_q}{S}\cos(k_s s)$	$\int_0^s ds\,\beta_q(s)$	$\frac{\lambda_q S}{(2\pi)^2}[1 - \cos(k_s s)]$
$\beta_q(s)$	$-\frac{\lambda_q}{2\pi}\sin(k_s s)$	$\int_0^s ds[\delta_q(s) - \langle\delta_q\rangle]$	$-\frac{\lambda_q^2}{2\pi S}[\frac{1}{4}\sin(2k_s s) + 2\sin(k_s s)]$
$\langle\beta_q\rangle$	0	$\kappa_{fq}S^2$	$\frac{3}{2}\lambda_q^2$

3. Coordinate transformation for an alternating-gradient quadrupole field

We make use of Eqs. (39), (40), (47), (48), (60), and (61) to evaluate $x(X,Y,X',Y',s) = X + \epsilon x_1 + \epsilon^2 x_2 + \epsilon^3 x_3 + \cdots$, etc., for an alternating-gradient quadrupole field with $\kappa_q(s + S) = \kappa_q(s)$ and $S^{-1}\int_0^S ds\, \kappa_q(s) = 0$. Making use of the symmetries in Eq. (65) and setting $\epsilon = 1$, we obtain, correct to third order in ϵ,

$$
\begin{aligned}
x(X,Y,X',Y',s) &= X - \beta_q(s)X + 2\left[\int_0^s ds\, \beta_q(s)\right]X', \\
y(X,Y,X',Y',s) &= Y + \beta_q(s)Y - 2\left[\int_0^s ds\, \beta_q(s)\right]Y',
\end{aligned}
\tag{71}
$$

and

$$
\begin{aligned}
x'(X,Y,X',Y',s) = X' - \alpha_q(s)X + \beta_q(s)X' + \left[\int_0^s ds\, \beta_q(s)\right]\frac{\partial}{\partial X}\left(X\frac{\partial\psi}{\partial X} - Y\frac{\partial\psi}{\partial Y}\right) \\
- \left(\int_0^s ds[\delta_q(s) - \langle\delta_q\rangle]\right)X - \alpha_q(s)\beta_q(s)X\,, \\
y'(X,Y,X',Y',s) = Y' + \alpha_q(s)Y - \beta_q(s)Y' - \left[\int_0^s ds\, \beta_q(s)\right]\frac{\partial}{\partial Y}\left(Y\frac{\partial\psi}{\partial Y} - X\frac{\partial\psi}{\partial X}\right) \\
- \left(\int_0^s ds[\delta_q(s) - \langle\delta_q\rangle]\right)Y - \alpha_q(s)\beta_q(s)Y\,.
\end{aligned}
\tag{72}
$$

Here, the coefficients in Eqs. (71) and (72) are defined in Eq. (67). Moreover, the terms in Eqs. (71) and (72) proportional to $\alpha_q(s)$, $\beta_q(s)$, $\int_0^s ds\, \beta_q(s)$, $\int_0^s ds[\delta_q(s) - \langle\delta_q\rangle]$, and $\alpha_q(s)\beta_q(s)$ are of order ϵ, ϵ^2, ϵ^3, ϵ^3, and ϵ^3, respectively. In Eq. (72), note that use has been made of $\bar{\kappa}_x = -\bar{\kappa}_y = S^{-1}\int_0^S ds\, \kappa_q(s) = 0$ for a periodic quadrupole field.

4. Coordinate transformation for a periodic-focusing solenoidal field

Finally, we make use of Eqs. (39), (40), (47), (48), (60), and (61) to evaluate $x(X,Y,X',Y',s) = X + \epsilon x_1 + \epsilon^2 x_2 + \epsilon^3 x_3 + \cdots$, etc., for a periodic-focusing solenoidal field with $\kappa_s(s + S) = \kappa_s(s)$ and $S^{-1}\int_0^S ds\, \kappa_s(s) = \bar{\kappa}_s \neq 0$. Correct to order ϵ^3, making use of the symmetries in Eq. (69) and setting $\epsilon = 1$, we readily obtain

$$
\begin{aligned}
x(X,Y,X',Y',s) &= X - \beta_s(s)X + 2\left[\int_0^s ds\, \beta_s(s))\right]X', \\
y(X,Y,X',Y',s) &= Y - \beta_s(s)Y + 2\left[\int_0^s ds\, \beta_s(s)\right]Y',
\end{aligned}
\tag{73}
$$

and

$$
\begin{aligned}
x'(X,Y,X',Y',s) = X' - \alpha_s(s)X + \beta_s(s)X' + \left[\int_0^s ds\, \beta_s(s)\right]\left[2\bar{\kappa}_s X + \frac{\partial}{\partial X}\left(X\frac{\partial\psi}{\partial X} + Y\frac{\partial\psi}{\partial Y}\right)\right] \\
- \left(\int_0^s ds[\delta_s(s) - \langle\delta_s\rangle]\right)X - \alpha_s(s)\beta_s(s)X\,, \\
y'(X,Y,X',Y',s) = Y' - \alpha_s(s)Y + \beta_s(s)Y' + \left[\int_0^s ds\, \beta_s(s)\right]\left[2\bar{\kappa}_s Y + \frac{\partial}{\partial Y}\left(X\frac{\partial\psi}{\partial X} + Y\frac{\partial\psi}{\partial Y}\right)\right] \\
- \left(\int_0^s ds[\delta_s(s) - \langle\delta_s\rangle]\right)Y - \alpha_s(s)\beta_s(s)Y\,.
\end{aligned}
\tag{74}
$$

Here, the coefficients in Eqs. (73) and (74) are defined in Eq. (69). In addition, the terms in Eqs. (73) and (74) proportional to $\alpha_s(s)$, $\beta_s(s)$, $\int_0^s ds\, \beta_s(s)$, $\int_0^s ds[\delta_s(s) - \langle\delta_s\rangle]$, and $\alpha_s(s)\beta_s(s)$ are of order ϵ, ϵ^2, ϵ^3, ϵ^3, and ϵ^3, respectively. Finally, as expected, it is evident from Eqs. (73) and (74) that there is a high degree of symmetry in the x and y motions for the case of a periodic-focusing solenoidal field.

In concluding this section, for the case of a periodic-focusing solenoidal field, we demonstrate an important check on Eqs. (73) and (74) related to the conservation of canonical angular momentum [21]. In laboratory-frame variables (actually Larmor-frame variables) the normalized canonical angular momentum is defined by $P_\theta = xy' - yx'$. Expressing $x = X + \epsilon x_1 + \epsilon^2 x_2 + \epsilon^3 x_3 + \cdots$, $y' = Y' + \epsilon y_1' + \epsilon^2 y_2' + \epsilon^3 y_3' + \cdots$, etc., and making use of $x_1 = 0 = y_1$, the canonical angular momentum can be expressed as

$$P_\theta = xy' - yx' = XY' - YX' + \epsilon(Xy_1' - Yx_1') + \epsilon^2(Xy_2' - Yx_2' + x_2Y' - y_2X') + \epsilon^3(Xy_3' - Yx_3' + x_3Y' - y_3X' + x_2y_1' - y_1x_2') + O(\epsilon^4). \quad (75)$$

Some straightforward algebra that makes use of Eqs. (73)–(75) gives

$$P_\theta = XY' - YX' + \left[\int_0^s ds\,\beta_s(s)\right]\left(X\frac{\partial}{\partial Y} - Y\frac{\partial}{\partial X}\right) \times \left(X\frac{\partial\psi}{\partial X} + Y\frac{\partial\psi}{\partial Y}\right) + O(\epsilon^4), \quad (76)$$

where $XY' = YX' = P_\Theta$ is the canonical angular momentum in the slow variables. An important conclusion is immediately evident from Eq. (76). We denote $X = R\cos\Theta$ and $Y = R\sin\Theta$, where $R = (X^2 + Y^2)^{1/2}$. Then $(X\partial/\partial X + Y\partial/\partial Y)\psi(X,Y,s) = R(\partial/\partial R)\psi(R,\Theta,s)$ and $X\partial/\partial Y - Y\partial/\partial X = \partial/\partial\Theta$. Equation (76) then reduces to

$$P_\theta = P_\Theta + \left[\int_0^s ds\,\beta_s(s)\right] R\frac{\partial}{\partial R}\frac{\partial}{\partial\Theta}\psi(R,\Theta,s), \quad (77)$$

correct to order ϵ^3. Therefore, as expected, when $\psi(R,\Theta,s)$ is axisymmetric in the transformed variables with $\partial\psi/\partial\Theta = 0$, it follows that

$$P_\theta = P_\Theta = \text{const} \quad (\text{independent of } s), \quad (78)$$

corresponding to conservation of canonical angular momentum [12,21].

IV. NONLINEAR VLASOV-MAXWELL EQUATIONS IN THE SLOW VARIABLES

In this section, we examine properties of the nonlinear Vlasov-Maxwell equations for $F_b(X,Y,X',Y',s)$ and $\psi(X,Y,s)$ in the slow phase space variables (Sec. IV A) and present several examples of equilibrium solutions $F_b^0(\mathcal{H}^0)$ with $\partial/\partial s = 0$ (Sec. IV B). The coordinate transformations in Eqs. (71) and (72) (periodic quadrupole field) and in Eqs. (73) and (74) (periodic solenoidal field) are then used in Sec. V to examine statistical averages and key properties of the periodically focused ion beam distribution $f_b(x,y,x',y',s)$ in laboratory-frame variables. For completeness, the linearized Vlasov-Maxwell equations in the transformed variables are presented in Sec. IV C.

A. Transformed Hamiltonian and nonlinear Vlasov-Maxwell equations in the slow variables

For present purposes, it is convenient to work with the slow variables $(\tilde{X},\tilde{Y},\tilde{X}',\tilde{Y}')$ which are related to (X,Y,X',Y') by the fiber transformation [38] in Eq. (65). In this case, making use of Eqs. (66), (68), and (70), the transformed Hamiltonian in the slow variables $(\tilde{X},\tilde{Y},\tilde{X}',\tilde{Y}')$ can be expressed as

$$\mathcal{H}(\tilde{X},\tilde{Y},\tilde{X}',\tilde{Y}',s) = \frac{1}{2}(\tilde{X}'^2 + \tilde{Y}'^2) + \frac{1}{2}\kappa_f(\tilde{X}^2 + \tilde{Y}^2) + \psi(\tilde{X},\tilde{Y},s), \quad (79)$$

correct to order ϵ^3. Here, for the case of a periodic-focusing quadrupole field, $(\tilde{X},\tilde{Y},\tilde{X}',\tilde{Y}')$ and κ_f are defined by

$$\begin{aligned}\tilde{X} &= X, & \tilde{Y} &= Y,\\ \tilde{X}' &= X' - \langle\alpha_q\rangle X, & \tilde{Y}' &= Y' + \langle\alpha_q\rangle Y,\\ \kappa_f \equiv \kappa_{fq} &= \frac{3}{S}\int_0^S ds[\alpha_q^2(s) - \langle\alpha_q\rangle^2],\end{aligned} \quad (80)$$

where use has been made of Eqs. (65), (67), and (68). On the other hand, for the case of a periodic-focusing solenoidal field, $(\tilde{X},\tilde{Y},\tilde{X}',\tilde{Y}')$ and κ_f are defined by

$$\begin{aligned}\tilde{X} &= X, & \tilde{Y} &= Y,\\ \tilde{X}' &= X' - \langle\alpha_s\rangle X, & \tilde{Y}' &= Y' - \langle\alpha_s\rangle Y,\\ \kappa_f \equiv \bar{\kappa}_s + \kappa_{fs} &= \bar{\kappa}_s + \frac{3}{S}\int_0^S ds[\alpha_s^2(s) - \langle\alpha_s\rangle^2],\end{aligned} \quad (81)$$

where use has been made of Eqs. (65), (69), and (70).

The major simplification associated with transforming to the slow variables $(\tilde{X},\tilde{Y},\tilde{X}',\tilde{Y}')$ is immediately evident from Eq. (79). In particular, the focusing coefficient κ_f occurring in Eq. (79) is both *constant* (independent of s) and *isotropic* in the transverse plane. This should be contrasted with the expression for the Hamiltonian $\hat{H}(x,y,x',y',s)$ in the laboratory frame defined in Eq. (6), where the focusing coefficients $\kappa_x(s)$ and $\kappa_y(s)$ are rapidly oscillating functions of s.

For the Hamiltonian defined in Eq. (79), the single-particle equations of motion are given by

$$\begin{aligned}\frac{d}{ds}\tilde{\mathbf{X}} &= \frac{\partial\mathcal{H}}{\partial\tilde{\mathbf{X}}'} = \tilde{X}'\hat{\mathbf{e}}_x + \tilde{Y}'\hat{\mathbf{e}}_y,\\ \frac{d}{ds}\tilde{\mathbf{X}}' &= -\frac{\partial\mathcal{H}}{\partial\tilde{\mathbf{X}}} = -\kappa_f(\tilde{X}\hat{\mathbf{e}}_x + \tilde{Y}\hat{\mathbf{e}}_y) - \frac{\partial}{\partial\tilde{\mathbf{X}}}\psi(\tilde{X},\tilde{Y},s),\end{aligned} \quad (82)$$

and the nonlinear Vlasov equation for $F_b(\tilde{X},\tilde{Y},\tilde{X}',\tilde{Y}',s)$ can be expressed as

$$\left\{\frac{\partial}{\partial s} + \tilde{X}'\frac{\partial}{\partial \tilde{X}} + \tilde{Y}'\frac{\partial}{\partial \tilde{Y}} - \left(\kappa_f \tilde{X} + \frac{\partial}{\partial \tilde{X}}\psi\right)\frac{\partial}{\partial \tilde{X}'} - \left(\kappa_f \tilde{Y} + \frac{\partial}{\partial \tilde{Y}}\psi\right)\frac{\partial}{\partial \tilde{Y}'}\right\}F_b(\tilde{X},\tilde{Y},\tilde{X}',\tilde{Y}',s) = 0\,, \tag{83}$$

where $\kappa_f =$ const is defined in Eqs. (80) and (81). Comparing Eqs. (82) and (83), note that the characteristics of the Vlasov equation (83) correspond to the single-particle equations of motion in the transformed variables. For example, the coefficient of $\partial/\partial\tilde{X}$ is $d\tilde{X}/ds = \tilde{X}'$, the coefficient of $\partial/\partial\tilde{X}'$ is $d\tilde{X}'/ds = -\kappa_f\tilde{X} - \partial\psi/\partial\tilde{X}$, etc. The slowly varying self-field potential $\psi(\tilde{X},\tilde{Y},s)$ occurring in Eq. (83) is determined self-consistently in terms of the distribution function $F_b(\tilde{X},\tilde{Y},\tilde{X}',\tilde{Y}',s)$ from

$$\left(\frac{\partial^2}{\partial\tilde{X}^2} + \frac{\partial^2}{\partial\tilde{Y}^2}\right)\psi(\tilde{X},\tilde{Y},s) = -\frac{2\pi K_b}{N_b}\int d\tilde{X}'\,d\tilde{Y}' \times F_b(\tilde{X},\tilde{Y},\tilde{X}',\tilde{Y}',s)\,, \tag{84}$$

which should be compared with Eq. (4).

The nonlinear Vlasov-Maxwell equations (83) and (84) can be used to investigate detailed equilibrium and stability properties in the slow variables $(\tilde{X},\tilde{Y},\tilde{X}',\tilde{Y}')$ over a wide range of system parameters [12,21], including beam intensity (K_b), focusing-field strength (κ_f), and choices of equilibrium distribution function $F_b^0(\mathcal{H}^0)$, consistent with the assumption that the phase advance is sufficiently small [34] to assure good convergence of the averaging technique leading to Eq. (79). Of course, to determine properties of the (periodically focused) beam in the laboratory frame, use will be made of the back-transformation to the laboratory-frame coordinates (x,y,x',y') defined in Eqs. (71) and (72) (periodic-focusing quadrupole field) or in Eqs. (73) and (74) (periodic-focusing solenoidal field).

For simplicity, in the subsequent analysis of Eqs. (83) and (84), we employ free boundary conditions in which the conducting wall is assumed to be infinitely far removed from the ion beam in the transverse plane. Two points are especially noteworthy in this regard. First, while the variables $(\tilde{X},\tilde{Y})$ are *spacelike* and the variables $(\tilde{X}',\tilde{Y}')$ are *velocitylike* in a formal analysis of Eqs. (83) and (84), it is clear that the back-transformation to the laboratory-frame coordinates defined in Eqs. (71) and (72), or in Eqs. (73) and (74), inexorably *mixes* the dependence of (x,y,x',y') on the variables $(\tilde{X},\tilde{Y},\tilde{X}',\tilde{Y}')$. Second, a rigid conducting boundary in the laboratory frame will typically have a pulsating (s-dependent) shape in the transformed variables. For example, consider the coordinate transformation for a periodic-focusing quadrupole field given in Eqs. (71) and (72). Correct to order ϵ^2, Eq. (71) gives $x = [1-\beta_q(s)]\tilde{X}$ and $y = [1+\beta_q(s)]\tilde{Y}$. Therefore, a circular cross-section conducting wall with constant radius $(x^2+y^2)^{1/2} = r_w =$ const in the laboratory frame corresponds to a pulsating conducting wall with elliptical cross section, $\tilde{X}^2/a_w^2(s) + \tilde{Y}^2/b_w^2(s) = 1$, in the transformed variables, where $a_w^2(s) = r_w^2/[1-\beta_q(s)]^2$ and $b_w^2(s) = r_w^2/[1+\beta_q(s)]^2$. As noted earlier, the subsequent analysis in Secs. IV and V effectively assumes that the conducting wall is infinitely far removed from the beam $(r_w \to \infty)$.

In concluding this section, it is important to emphasize that the nonlinear Vlasov-Maxwell equations (83) and (84) in the slow variables $(\tilde{X},\tilde{Y},\tilde{X}',\tilde{Y}')$, when supplemented by the coordinate transformations in Eqs. (71) and (72) (periodic-focusing quadrupole field) or in Eqs. (73) and (74) (periodic-focusing solenoidal field), are fully equivalent to the nonlinear Vlasov-Maxwell equations (3) and (4) in the laboratory-frame variables (x,y,x',y') correct to order ϵ^3. In this regard, because the coordinate transformation is canonical, the laboratory-frame distribution function $f_b(x,y,x',y',s)$ is related to the transformed distribution function $F_b(\tilde{X},\tilde{Y},\tilde{X}',\tilde{Y}',s)$ by

$$f_b(x,y,x',y',s)dxdydx'dy' = F_b(\tilde{X},\tilde{Y},\tilde{X}',\tilde{Y}',s) \times d\tilde{X}d\tilde{Y}d\tilde{X}'d\tilde{Y}', \tag{85}$$

and the Jacobian of the transformation is equal to unity; i.e.,

$$\frac{\partial(x,y,x',y')}{\partial(\tilde{X},\tilde{Y},\tilde{X}',\tilde{Y}')} = 1\,. \tag{86}$$

A direct calculation that makes use of Eqs. (71) and (72), or Eqs. (73) and (74), appropriately expressed in terms of the variables $(\tilde{X},\tilde{Y},\tilde{X}',\tilde{Y}')$ defined in Eqs. (80) and (81) shows that Eq. (86) is indeed satisfied correct to order ϵ^3.

For completeness and future reference in Sec. V, we record here the coordinate transformations relating (x,y,x',y') to $(\tilde{X},\tilde{Y},\tilde{X}',\tilde{Y}')$. For the case of a periodic-focusing quadrupole field, making use of Eqs. (71), (72), and (80), we obtain

$$\begin{aligned} x(\tilde{X},\tilde{Y},\tilde{X}',\tilde{Y}',s) &= [1-\beta_q(s)]\tilde{X} + 2\left[\int_0^s ds\,\beta_q(s)\right]\tilde{X}', \\ y(\tilde{X},\tilde{Y},\tilde{X}',\tilde{Y}',s) &= [1+\beta_q(s)]\tilde{Y} - 2\left[\int_0^s ds\,\beta_q(s)\right]\tilde{Y}', \end{aligned} \tag{87}$$

and

$$
\begin{aligned}
x'(\tilde{X},\tilde{Y},\tilde{X}',\tilde{Y}',s) &= [1+\beta_q(s)]\tilde{X}' + \left\{-\alpha_q(s) + \langle\alpha_q\rangle + \langle\alpha_q\rangle\beta_q(s) - \alpha_q(s)\beta_q(s) - \left(\int_0^s ds[\delta_q(s) - \langle\delta_q\rangle]\right)\right\}\tilde{X} \\
&\quad + \left[\int_0^s ds\,\beta_q(s)\right]\frac{\partial}{\partial\tilde{X}}\left(\tilde{X}\frac{\partial\psi}{\partial\tilde{X}} - \tilde{Y}\frac{\partial\psi}{\partial\tilde{Y}}\right), \\
y'(\tilde{X},\tilde{Y},\tilde{X}',\tilde{Y}',s) &= [1-\beta_q(s)]\tilde{Y}' + \left\{\alpha_q(s) - \langle\alpha_q\rangle + \langle\alpha_q\rangle\beta_q(s) - \alpha_q(s)\beta_q(s) - \left(\int_0^s ds[\delta_q(s) - \langle\delta_q\rangle]\right)\right\}\tilde{Y} \\
&\quad - \left[\int_0^s ds\,\beta_q(s)\right]\frac{\partial}{\partial\tilde{Y}}\left(\tilde{Y}\frac{\partial\psi}{\partial\tilde{Y}} - \tilde{X}\frac{\partial\psi}{\partial\tilde{X}}\right),
\end{aligned}
\tag{88}
$$

correct to order ϵ^3. In obtaining Eq. (87), we have neglected terms proportional to $\langle\alpha_q\rangle[\int_0^s ds\,\beta_q(s)]$, which are of order ϵ^4. Similarly, for the case of a periodic-focusing solenoidal field, making use of Eqs. (72), (73), and (81), we obtain

$$
\begin{aligned}
x(\tilde{X},\tilde{Y},\tilde{X}',\tilde{Y}',s) &= [1-\beta_s(s)]\tilde{X} + 2\left[\int_0^s ds\,\beta_s(s)\right]\tilde{X}', \\
y(\tilde{X},\tilde{Y},\tilde{X}',\tilde{Y}',s) &= [1-\beta_s(s)]\tilde{Y} + 2\left[\int_0^s ds\,\beta_s(s)\right]\tilde{Y}',
\end{aligned}
\tag{89}
$$

and

$$
\begin{aligned}
x'(\tilde{X},\tilde{Y},\tilde{X}',\tilde{Y}',s) = {} & [1+\beta_s(s)]\tilde{X}' + \Bigg\{-\alpha_s(s) + \langle\alpha_s\rangle + \langle\alpha_s\rangle\beta_s(s) - \alpha_s(s)\beta_s(s) - \left(\int_0^s ds[\delta_s(s) - \langle\delta_s\rangle]\right) \\
& + 2\bar{\kappa}_s\left[\int_0^s ds\,\beta_s(s)\right]\Bigg\}\tilde{X} + \left[\int_0^s ds\,\beta_s(s)\right]\frac{\partial}{\partial\tilde{X}}\left(\tilde{X}\frac{\partial\psi}{\partial\tilde{X}} + \tilde{Y}\frac{\partial\psi}{\partial\tilde{Y}}\right), \\
y'(\tilde{X},\tilde{Y},\tilde{X}',\tilde{Y}',s) = {} & [1+\beta_s(s)]\tilde{Y}' + \Bigg\{-\alpha_s(s) + \langle\alpha_s\rangle + \langle\alpha_s\rangle\beta_s(s) - \alpha_s(s)\beta_s(s) - \left(\int_0^s ds[\delta_s(s) - \langle\delta_s\rangle]\right) \\
& + 2\bar{\kappa}_s\left[\int_0^s ds\,\beta_s(s)\right]\Bigg\}\tilde{Y} + \left[\int_0^s ds\,\beta_s(s)\right]\frac{\partial}{\partial\tilde{Y}}\left(\tilde{X}\frac{\partial\psi}{\partial\tilde{X}} + \tilde{Y}\frac{\partial\psi}{\partial\tilde{Y}}\right),
\end{aligned}
\tag{90}
$$

correct to order ϵ^3. In obtaining Eq. (89), we have neglected terms proportional to $\langle\alpha_s\rangle[\int_0^s ds\,\beta_s(s)]$, which are of order ϵ^4. Finally, it should be noted that the slowly varying self-field potential $\psi(\tilde{X},\tilde{Y},s)$ occurring in the final terms in Eqs. (88) and (90) is to be determined self-consistently in terms of $F_b(\tilde{X},\tilde{Y},\tilde{X}',\tilde{Y}',s)$ from Eqs. (83) and (84).

The coordinate transformations in Eqs. (87)–(90) relate the laboratory-frame coordinates $x(\tilde{X},\tilde{Y},\tilde{X}',\tilde{Y}',s)$, $y(\tilde{X},\tilde{Y},\tilde{X}',\tilde{Y}',s)$, etc., directly to the slow variables $(\tilde{X},\tilde{Y},\tilde{X}',\tilde{Y}')$. In this regard, it is important to keep in mind the size of the various terms in Eqs. (87)–(90). In particular, referring to the analysis in Sec. III, the relative size of the terms in Eqs. (87)–(90) is specified by

$$
\begin{aligned}
\alpha_j(s),\ \langle\alpha_j\rangle: &\quad \text{Terms of order } \epsilon\,, \\
\beta_j(s): &\quad \text{Terms of order } \epsilon^2, \\
\langle\alpha_j\rangle\beta_j(s),\ \alpha_j(s)\beta_j(s),\ \left[\int_0^s ds\,\beta_j(s)\right],\ \left(\int_0^s ds[\delta_j(s) - \langle\delta_j\rangle]\right): &\quad \text{Terms of order } \epsilon^3,
\end{aligned}
\tag{91}
$$

where $j = q$ $(j = s)$ refers to the quadrupole (solenoidal) focusing case. It will also be useful in Sec. V to make use of the *inverse* transformation to Eqs. (87)–(90), which expresses the slow coordinates $\tilde{X}(x,y,x',y',s)$, $\tilde{Y}(x,y,x',y',s)$, etc., directly in terms of the laboratory-frame variables (x,y,x',y'). For completeness, the inverse coordinate transformation is presented correct to order ϵ^3 in the Appendix.

B. Equilibrium solutions ($\partial/\partial s = 0$) in the transformed variables

Because of the simple form of Eqs. (83) and (84), with constant focusing coefficient $\kappa_f = \text{const}$, the nonlinear Vlasov-Maxwell equations in the slow variables $(\tilde{X},\tilde{Y},\tilde{X}',\tilde{Y}')$ support a broad class of equilibrium solutions (denoted by F_b^0 and ψ^0) for which $\partial/\partial s = 0$ [12,21]. We introduce the cylindrical polar coordinates $(\tilde{R}, \Theta)$ defined by $\tilde{X} = \tilde{R}\cos\Theta$ and $\tilde{Y} = \tilde{R}\sin\Theta$, where $\tilde{R} = (\tilde{X}^2 + \tilde{Y}^2)^{1/2}$ is the effective radial coordinate in the slow variables. Because the focusing potential in Eq. (79) is of the form $(1/2)\kappa_f(\tilde{X}^2 + \tilde{Y}^2) = (1/2)\kappa_f\tilde{R}^2$, the nonlinear Vlasov-Maxwell equations (83) and (84) support axisymmetric equilibrium solutions with $\partial/\partial\Theta = 0$ and $\partial/\partial s = 0$ in which $F_b^0(\tilde{X}, \tilde{Y}, \tilde{X}', \tilde{Y}')$ and $\psi^0(\tilde{X}, \tilde{Y})$ depend on $\tilde{X}$ and $\tilde{Y}$ exclusively through the radial coordinate $\tilde{R} = (\tilde{X}^2 + \tilde{Y}^2)^{1/2}$. Specifically, because $\partial\psi^0/\partial\Theta = 0$ and $\partial\psi^0/\partial s = 0$, the transformed Hamiltonian $\mathcal{H}^0(\tilde{X}, \tilde{Y}, \tilde{X}', \tilde{Y}')$ for transverse particle motion in the equilibrium field configuration is given by

$$\mathcal{H}^0(\tilde{X}, \tilde{Y}, \tilde{X}', \tilde{Y}') = \frac{1}{2}(\tilde{X}'^2 + \tilde{Y}'^2) + \frac{1}{2}\kappa_f\tilde{R}^2 + \psi^0(\tilde{R}), \tag{92}$$

where $\mathcal{H}^0$ is exactly conserved ($d\mathcal{H}^0/ds = 0$) because $\partial\psi^0/\partial s = 0$.

The nonlinear Vlasov-Maxwell equations (83) and (84) support a broad class of equilibrium solutions ($\partial/\partial s = 0$) in which the equilibrium distribution function F_b^0 depends on the variables $(\tilde{X}, \tilde{Y}, \tilde{X}', \tilde{Y})$ exclusively through the Hamiltonian $\mathcal{H}^0$; i.e.,

$$F_b^0(\tilde{X}, \tilde{Y}, \tilde{X}', \tilde{Y}') = F_b^0(\mathcal{H}^0). \tag{93}$$

Here, $\mathcal{H}^0(\tilde{X}, \tilde{Y}, \tilde{X}', \tilde{Y}')$ is defined in Eq. (92). Substituting Eq. (93) into Eq. (83), it is readily shown that

$$\left\{\tilde{X}'\frac{\partial}{\partial\tilde{X}} + \tilde{Y}'\frac{\partial}{\partial\tilde{Y}} - \left(\kappa_f\tilde{X} + \frac{\tilde{X}}{\tilde{R}}\frac{\partial\psi^0}{\partial\tilde{R}}\right)\frac{\partial}{\partial\tilde{X}'} - \left(\kappa_f\tilde{Y} + \frac{\tilde{Y}}{\tilde{R}}\frac{\partial\psi^0}{\partial\tilde{R}}\right)\frac{\partial}{\partial\tilde{Y}'}\right\}F_b^0(\mathcal{H}^0) = 0 \tag{94}$$

is an *exact* consequence of Eq. (92), where use can be made of the chain rule for differentiation to express $\partial F_b^0/\partial\tilde{X}' = \tilde{X}'\partial F_b^0/\partial\mathcal{H}^0$, $(\partial/\partial\tilde{X})F_b^0 = [\kappa_f\tilde{X} + (\tilde{X}/\tilde{R})\partial\psi^0/\partial\tilde{R}]\partial F_b^0/\partial\mathcal{H}^0$, etc. Here, we have expressed $(\partial/\partial\tilde{X})\psi^0(\tilde{R}) = (\tilde{X}/\tilde{R})(\partial/\partial\tilde{R})\psi^0(\tilde{R})$, etc. Because $\partial\psi^0/\partial\Theta = 0$, the canonical angular momentum $P_\Theta = \tilde{X}\tilde{Y}' - \tilde{Y}\tilde{X}'$ is also an exact single-particle constant of the motion ($dP_\Theta/ds = 0$) in the transformed variables. Therefore, more generally speaking, the equilibrium distribution function $F_b^0(\mathcal{H}^0, P_\Theta)$ could also depend explicitly on P_Θ as well as $\mathcal{H}^0$ [12,21]. Such beam equilibria are typically rotating and will not be considered in the present analysis.

There is clearly enormous latitude in specifying the functional form of the equilibrium distribution function $F_b^0(\mathcal{H}^0)$ in the transformed variables [12]. Once the form of $F_b^0(\mathcal{H}^0)$ is specified, however, the corresponding equilibrium self-field potential $\psi^0(R)$ is to be calculated self-consistently from Eq. (84). For $\partial/\partial\Theta = 0$ and $\partial/\partial s = 0$, Eq. (84) becomes

$$\frac{1}{\tilde{R}}\frac{\partial}{\partial\tilde{R}}\tilde{R}\frac{\partial}{\partial\tilde{R}}\psi^0(\tilde{R}) = -\frac{2\pi K_b}{N_b}\int d\tilde{X}'\,d\tilde{Y}'\,F_b^0(\mathcal{H}^0), \tag{95}$$

where $\mathcal{H}^0$ is defined in Eq. (92), and

$$n_b^0(\tilde{R}) = \int d\tilde{X}'\,d\tilde{Y}'\,F_b^0(\mathcal{H}^0) \tag{96}$$

is the radial density profile in the transformed variables. Because $\mathcal{H}^0$ depends explicitly on $\psi^0(\tilde{R})$ [Eq. (92)], the Maxwell equation (95) is generally a *nonlinear* differential equation for the self-field potential $\psi^0(\tilde{R})$. Expressing $\tilde{U} = (1/2)(\tilde{X}'^2 + \tilde{Y}'^2)$ and $\mathcal{H}^0 = \tilde{U} + \kappa_f\tilde{R}^2/2 + \psi^0(\tilde{R})$, and converting the velocity integration range in Eqs. (95) and (96) according to $\int_{-\infty}^{\infty} d\tilde{X}'\int_{-\infty}^{\infty} d\tilde{Y}'\cdots = 2\pi\int_0^\infty d\tilde{U}\cdots$, the equilibrium density profile $n_b^0(\tilde{R})$ in the transformed variables can be expressed in the equivalent form

$$n_b^0(\tilde{R}) = 2\pi\int_0^\infty d\tilde{U}\,F_b^0[\tilde{U} + \kappa_f\tilde{R}^2/2 + \psi^0(\tilde{R})]. \tag{97}$$

Other equilibrium properties are also readily calculated in terms of $F_b^0(\mathcal{H}^0)$. For example, in the transformed variables, because $\mathcal{H}^0$ is an even function of $\tilde{X}'$ and $\tilde{Y}'$, the average local flow velocity in the transverse plane is equal to zero; i.e., $\mathbf{V}_b^0(\tilde{\mathbf{X}}) \equiv [n_b^0(\tilde{R})]^{-1}\beta_b c\int d\tilde{X}'\,d\tilde{Y}'(\tilde{X}'\hat{\mathbf{e}}_x + \tilde{Y}'\hat{\mathbf{e}}_y)F_b^0(\mathcal{H}^0) = 0$. Moreover, the effective perpendicular temperature $T_{\perp b}^0(\tilde{R})$ in the transformed variables is defined (in energy units) by

$$\begin{aligned} n_b^0(\tilde{R})T_{\perp b}^0(\tilde{R}) &= \int d\tilde{X}'\,d\tilde{Y}'\,\frac{1}{2}\gamma_b m_b\beta_b^2c^2(\tilde{X}'^2 + \tilde{Y}'^2)F_b^0(\mathcal{H}^0) \\ &= 2\pi\gamma_b m_b\beta_b^2c^2\int_0^\infty d\tilde{U}\,\tilde{U}F_b^0[\tilde{U} + \kappa_f\tilde{R}^2/2 + \psi^0(\tilde{R})], \end{aligned} \tag{98}$$

where $\tilde{U} = (1/2)(\tilde{X}'^2 + \tilde{Y}'^2)$.

The general class of equilibrium distribution functions described by Eqs. (92) and (93) corresponds to an intense charged particle beam with circular cross section confined in the transverse plane by a uniform focusing force ($\kappa_f =$ const). This class of distribution functions $F_b^0(\mathcal{H}^0)$ has been extensively analyzed in the literature [12,16,17,21]. For present purposes, we summarize here several key properties of the equilibrium and give specific examples of beam equilibria $F_b^0(\mathcal{H}^0)$ in the transformed variables. These results will be very useful in Sec. V when we transform back to the laboratory frame where the beam properties are periodically focused as a function of s.

1. Statistical averages

The statistical average of a phase function $\chi(\tilde{X},\tilde{Y},\tilde{X}',\tilde{Y}',s)$ over the equilibrium distribution function $F_b^0(\mathcal{H}^0)$ in the transformed variables is defined in the usual manner by

$$\langle\chi\rangle_0 = \frac{1}{N_b}\int d\tilde{X}\,d\tilde{Y}\,d\tilde{X}'\,d\tilde{Y}'\,\chi(\tilde{X},\tilde{Y},\tilde{X}',\tilde{Y}',s)F_b^0(\mathcal{H}^0)\,, \tag{99}$$

where $\mathcal{H}^0$ is defined in Eq. (92), and $N_b = \int d\tilde{X}\,d\tilde{Y}\,d\tilde{X}'\,d\tilde{Y}'\,F_b^0 = 2\pi\int_0^\infty d\tilde{R}\,\tilde{R}n_b^0(\tilde{R})$ is the number of beam particles per unit axial length. Because $\mathcal{H}^0(\tilde{X},\tilde{Y},\tilde{X}',\tilde{Y}')$ is an even function of $\tilde{X}$, $\tilde{Y}$, $\tilde{X}'$, and $\tilde{Y}'$, it follows that the statistical average of any odd power of $\tilde{X}$, $\tilde{Y}$, $\tilde{X}'$, or $\tilde{Y}'$, or products thereof, is equal to zero. For example, it follows that

$$\begin{aligned}\langle\tilde{X}\rangle_0 &= 0 = \langle\tilde{Y}\rangle_0\,,\\ \langle\tilde{X}'\rangle_0 &= 0 = \langle\tilde{Y}'\rangle_0\,,\\ \langle\tilde{X}\tilde{X}'\rangle_0 &= 0 = \langle\tilde{Y}\tilde{Y}'\rangle_0\,,\\ \langle\tilde{X}\tilde{Y}'\rangle_0 &= 0 = \langle\tilde{Y}\tilde{X}'\rangle_0\,,\end{aligned} \tag{100}$$

etc. Similarly, the rms beam radius R_{b0} and unnormalized beam emittance ϵ_0 in the transformed variables are defined by

$$\begin{aligned}R_{b0}^2 &= \langle\tilde{X}^2+\tilde{Y}^2\rangle_0\,,\\ \epsilon_0^2 &= 4\langle\tilde{X}'^2+\tilde{Y}'^2\rangle_0\langle\tilde{X}^2+\tilde{Y}^2\rangle_0\,,\end{aligned} \tag{101}$$

where R_{b0} and ϵ_0 are constants (independent of s) because $\partial F_b^0(\mathcal{H}^0)/\partial s = 0$. Because of the high degree of symmetry of $\mathcal{H}^0$, it also follows that

$$\begin{aligned}\langle\tilde{X}^2\rangle_0 &= \langle\tilde{Y}^2\rangle_0 = \frac{1}{2}\langle\tilde{X}^2+\tilde{Y}^2\rangle_0 = \frac{1}{2}R_{b0}^2\,,\\ \langle\tilde{X}'^2\rangle_0 &= \langle\tilde{Y}'^2\rangle_0 = \frac{1}{2}\langle\tilde{X}'^2+\tilde{Y}'^2\rangle_0\,.\end{aligned} \tag{102}$$

Finally, some straightforward algebra that makes use of Eqs. (98) and (101) shows that

$$\epsilon_0^2 = \frac{8R_{b0}^2}{N_b\gamma_b m_b\beta_b^2c^2}\,2\pi\int_0^\infty d\tilde{R}\,\tilde{R}n_b^0(\tilde{R})T_{\perp b}^0(\tilde{R})\,. \tag{103}$$

That is, ϵ_0^2 is directly proportional to the perpendicular pressure $P_{\perp b}^0(\tilde{R}) = n_b^0(\tilde{R})T_{\perp b}^0(\tilde{R})$, averaged over the radial cross section of the beam.

2. Radial force balance and envelope equation for the rms beam radius R_{b0}

The formal expression for the perpendicular pressure $P_{\perp b}^0(\tilde{R}) = n_b^0(\tilde{R})T_{\perp b}^0(\tilde{R})$ in Eq. (98) can be used to derive the equation for equilibrium radial force balance on a beam fluid element in the transformed variables. Taking the derivative of Eq. (98) with respect to $\tilde{R}$, it is readily shown that

$$\begin{aligned}\frac{\partial}{\partial\tilde{R}}P_{\perp b}^0 &= \gamma_b m_b\beta_b^2c^2\left(\kappa_f\tilde{R}+\frac{\partial\psi^0}{\partial\tilde{R}}\right)2\pi\int_0^\infty d\tilde{U}\,\tilde{U}\,\frac{\partial}{\partial\tilde{U}}F_b^0[\tilde{U}+\kappa_f\tilde{R}^2/2+\psi^0(\tilde{R})]\\ &= -\gamma_b m_b\beta_b^2c^2\left(\kappa_f\tilde{R}+\frac{\partial\psi^0}{\partial\tilde{R}}\right)2\pi\int_0^\infty d\tilde{U}\,F_b^0[\tilde{U}+\kappa_f\tilde{R}^2/2+\psi^0(\tilde{R})]\,,\end{aligned} \tag{104}$$

where we have integrated by parts with respect to $\tilde{U}$ and assumed $[F_b^0]_{\tilde{U}\to\infty} = 0$. Making use of $n_b^0(\tilde{R}) = 2\pi\int_0^\infty d\tilde{U}\,F_b^0[\tilde{U}+\kappa_f\tilde{R}^2/2+\psi^0(\tilde{R})]$, Eq. (104) can be expressed as

$$\frac{\partial}{\partial\tilde{R}}P_{\perp b}^0(\tilde{R}) = -\gamma_b m_b\beta_b^2c^2n_b^0(\tilde{R})\left[\kappa_f\tilde{R}+\frac{\partial}{\partial\tilde{R}}\psi^0(\tilde{R})\right], \tag{105}$$

which will be recognized as the equation for *local* radial force balance on a beam fluid element in the transformed variables. Solving Eq. (95) for $\partial\psi^0(\tilde{R})/\partial\tilde{R}$ in terms of the radial density profile $n_b^0(\tilde{R})$, Eq. (105) can also be expressed as [21]

$$\frac{\partial}{\partial\tilde{R}}P_{\perp b}^0(\tilde{R}) = -\gamma_b m_b\beta_b^2c^2n_b^0(\tilde{R})\times\left[\kappa_f\tilde{R}-\frac{2\pi K_b}{N_b}\frac{1}{\tilde{R}}\int_0^{\tilde{R}}d\tilde{R}\,\tilde{R}n_b^0(\tilde{R})\right]. \tag{106}$$

The local force balance Eq. (106) can be used to derive a *global* radial force balance equation that relates the emittance ϵ_0, the focusing coefficient κ_f, and the rms beam radius R_{b0}. To briefly summarize, we operate on Eq. (106) with $2\pi\int_0^\infty d\tilde{R}\,\tilde{R}^2\cdots$ and integrate by parts with respect to $\tilde{R}$, assuming $P_{\perp b}^0(\tilde{R}\to\infty) = 0 = n_b^0(\tilde{R}\to\infty)$. Some straightforward algebraic manipulation that makes use of Eq. (103) and $N_b = 2\pi\int_0^\infty d\tilde{R}\,\tilde{R}n_b^0(\tilde{R})$ readily gives the global force balance condition [21,24]

$$\left(\kappa_f-\frac{K_b}{2R_{b0}^2}\right)R_{b0} = \frac{\epsilon_0^2}{4R_{b0}^3}\,, \tag{107}$$

where $K_b = 2N_bZ_b^2e^2/\gamma_b^3m_b\beta_b^2c^2$ is the self-field perveance. Equation (107), valid for general choice of $F_b^0(\mathcal{H}^0)$, plays the role of an *envelope equation* for the rms beam radius R_{b0} and represents a powerful constraint condition on beam equilibrium properties [21]. As expected, if we make the identification $R_{b0} = r_{b0}/\sqrt{2}$, Eq. (107) is similar in form to the familiar envelope equation for the outer radius r_{b0} of a uniform-density KV beam equilibrium [10,11] in the smooth-beam approximation ($dr_{b0}/ds = 0$). For specified values of κ_f, K_b, and ϵ_0^2, note that Eq. (107) can be solved for the mean-square beam radius to give

$$R_{b0}^2 = \frac{K_b}{4\kappa_f} + \left[\left(\frac{K_b}{4\kappa_f}\right)^2 + \frac{\epsilon_0^2}{4\kappa_f}\right]^{1/2}. \tag{108}$$

As expected, we find from Eq. (108) that R_{b0}^2 increases with increasing beam intensity (K_b), increasing beam emittance (ϵ_0), and decreasing focusing-field strength (κ_f).

3. Phase advance σ_0

It is convenient to introduce the effective phase advance σ_0 over one lattice period S defined by $\sigma_0 = \epsilon_0 \int_0^S ds/2R_{b0}^2 = \epsilon_0 S/2R_{b0}^2$, where $R_{b0}^2 = \text{const}$ is the mean-square beam radius defined in Eq. (108). This gives

$$\sigma_0 = \frac{\sigma_{0v}}{[1 + (\frac{K_b}{2\sqrt{\kappa_f}\,\epsilon_0})^2]^{1/2} + (\frac{K_b}{2\sqrt{\kappa_f}\,\epsilon_0})}, \tag{109}$$

where $\sigma_{0v} = [\sigma_0]_{K_b \to 0} \equiv \sqrt{\kappa_f}\,S$ is the *vacuum* phase advance defined in the limit of negligible beam intensity, $K_b/\sqrt{\kappa_f}\,2\epsilon_0 \to 0$. As noted in Sec. I, the averaging technique developed in Sec. III is expected to provide good convergence properties [34] provided the phase advance σ_0 is sufficiently small ($\sigma_0 < 60° = \pi/3$, say). It is important to note from Eq. (109) that σ_0/σ_{0v} decreases monotonically from unity as the normalized beam intensity $K_b/2\sqrt{\kappa_f}\,\epsilon_0$ is increased. That is, self-field effects (as measured by K_b) *depress* the phase advance σ_0 from its vacuum value σ_{0v}.

4. Density inversion theorem and condition for transverse confinement

As noted earlier for the specified equilibrium distribution function $F_b^0(\mathcal{H}^0)$, when the expression for the density profile $n_b^0(\tilde{R})$ in Eq. (97) is substituted into Eq. (95), the resulting equation for the self-field potential $\psi^0(\tilde{R})$ is generally nonlinear. Without loss of generality, we take the zero of potential to be $\psi^0(\tilde{R} = 0) = 0$ and denote the on-axis value of beam density in the transformed variables by $n_b^0(\tilde{R} = 0) \equiv \hat{n}_b$. Integration of Eq. (95) from $\tilde{R} = 0$ readily gives $\psi^0(\tilde{R}) = -(\pi/2)(K_b\hat{n}_b/N_b)\tilde{R}^2$ for small values of $\tilde{R} \ll R_{b0}$. Careful examination of Eqs. (95) and (97) then shows that a necessary condition for a radially confined beam equilibrium with $n_b^0(\tilde{R} \to \infty) = 0$ is given by

$$\kappa_f \beta_b^2 c^2 > \frac{1}{2\gamma_b^2}\,\hat{\omega}_{pb}^2, \tag{110}$$

where $\hat{\omega}_{pb}^2 = 4\pi\hat{n}_b Z_b^2 e^2/\gamma_b m_b$ is the on-axis plasma frequency squared [12], and use has been made of the definition $K_b = 2N_b Z_b^2 e^2/\gamma_b^3 m_b \beta_b^2 c^2$. The inequality in Eq. (110) is simply a statement that the focusing force (proportional to $\kappa_f \beta_b^2 c^2$) must exceed the repulsive space-charge force (proportional to $\hat{\omega}_{pb}^2/2$) for there to be transverse confinement of the beam particles.

A further important result is evident from the expression for $n_b^0(\tilde{R})$ in Eq. (97). We introduce the effective total potential $V(\tilde{R})$ defined by $V(\tilde{R}) = (1/2)\kappa_f \tilde{R}^2 + \psi^0(\tilde{R})$. Then, taking the derivative of $n_b^0(V)$ with respect to V in Eq. (97) gives

$$\frac{\partial n_b^0}{\partial V} = 2\pi \int_0^\infty d\tilde{U}\,\frac{\partial}{\partial \tilde{U}} F_b^0[\tilde{U} + V(\tilde{R})]. \tag{111}$$

Assuming $F_b^0[\tilde{U} + V(\tilde{R})]_{\tilde{U}\to\infty} = 0$ and integrating by parts with respect to $\tilde{U}$ in Eq. (111) gives

$$F_b^0(\mathcal{H}^0) = -\frac{1}{2\pi}\left[\frac{\partial n_b^0}{\partial V}\right]_{V = \mathcal{H}^0} \tag{112}$$

for the distribution function $F_b^0(\mathcal{H}^0)$. Equation (112) is known as the *density inversion theorem* [1,21]. In particular, for specified density profile $n_b^0(\tilde{R})$, we make use of Eq. (95) to determine the self-field potential $\psi^0(\tilde{R})$ and evaluate the effective potential $V(\tilde{R}) = (1/2)\kappa_f \tilde{R}^2 + \psi^0(\tilde{R})$. Solving then for $\tilde{R}(V)$, assumed to be monotonic, we evaluate $\partial n_b^0/\partial V = (\partial n_b^0/\partial \tilde{R})(\partial \tilde{R}/\partial V)$ in Eq. (112), which determines the equilibrium distribution function $F_b^0(\mathcal{H}^0)$ in the transformed variables.

5. Kinetic stability theorem

An important kinetic stability theorem [25,26] can be demonstrated from the nonlinear Vlasov-Maxwell equations (83) and (84) for the distribution function $F_b(\tilde{X}, \tilde{Y}, \tilde{X}', \tilde{Y}', s)$ and self-field potential $\psi(\tilde{X}, \tilde{Y}, s)$. In particular, we express $F_b = F_b^0(\mathcal{H}^0) + \delta F_b(\tilde{X}, \tilde{Y}, \tilde{X}', \tilde{Y}', s)$ and $\psi = \psi^0(\tilde{R}) + \delta\psi(\tilde{X}, \tilde{Y}, s)$ and make use of the global conservation constraints for total energy $U(s)$ and generalized entropy $S(s)$ satisfied *exactly* by Eqs. (83) and (84); i.e.,

$$\begin{aligned} U(s) &= \int d\tilde{X}\,d\tilde{Y}\left\{\frac{N_b}{4\pi K_b}\,|\tilde{\nabla}\psi|^2 + \int d\tilde{X}'\,d\tilde{Y}'\left[\frac{1}{2}\,\kappa_f(\tilde{X}^2 + \tilde{Y}^2) + \frac{1}{2}\,(\tilde{X}'^2 + \tilde{Y}'^2)\right]F_b\right\} = \text{const}, \\ S(s) &= \int d\tilde{X}\,d\tilde{Y}\,d\tilde{X}'\,d\tilde{Y}'\,G(F_b) = \text{const}. \end{aligned} \tag{113}$$

Here, $dU/ds = 0 = dS/ds$, and $G(F_b)$ is a smooth, differentiable function of F_b with $G(F_b \to 0) = 0$. Without presenting algebraic details, it can be shown [25,26] that a *sufficient condition for stability* is that the equilibrium distribution function $F_b^0(\mathcal{H}^0)$ be a monotonically decreasing function of energy $\mathcal{H}^0$; i.e.,

$$\frac{\partial}{\partial \mathcal{H}^0} F_b^0(\mathcal{H}^0) \le 0 . \tag{114}$$

That is, whenever Eq. (114) is satisfied, the system is *stable*, and the perturbations $\delta\psi$ and δF_b do not amplify. The stability theorem in Eq. (114) is a very powerful result and is valid nonlinearly (finite-amplitude perturbations) as well as for small-amplitude perturbations. For example, Eq. (114) implies that a beam with thermal equilibrium [1,18,21] distribution $F_b^0(\mathcal{H}^0)$ [Eq. (115)] is stable and can propagate quiescently over large distances. On the other hand, a Kapchinskij-Vladimirskij beam equilibrium [Eq. (116)] has an inverted population in $\mathcal{H}^0$, and there is (in principle) free energy available to cause the perturbations $\delta\psi$ and δF_b to amplify [10–14].

6. Examples of self-consistent beam equilibria

For future reference, we briefly consider several examples of beam equilibria, $F_b^0(\mathcal{H}^0)$, in the transformed variables $(\tilde{X}, \tilde{Y}, \tilde{X}', \tilde{Y}')$. Specifically, we consider the following choices of $F_b^0(\mathcal{H}^0)$:

Thermal Equilibrium: [1,18,21]

$$F_b^0(\mathcal{H}^0) = \hat{n}_b \left(\frac{\gamma_b m_b \beta_b^2 c^2}{2\pi \hat{T}_{\perp b}} \right) \exp\left\{ -\frac{\gamma_b m_b \beta_b^2 c^2}{\hat{T}_{\perp b}} \mathcal{H}^0 \right\}, \tag{115}$$

Kapchinskij-Vladimirskij Equilibrium: [10–12,21]

$$F_b^0(\mathcal{H}^0) = \frac{\hat{n}_b}{2\pi} \delta(\mathcal{H}^0 - \hat{T}_{\perp b}/\gamma_b m_b \beta_b^2 c^2), \tag{116}$$

Waterbag Equilibrium: [16,17,21]

$$F_b^0(\mathcal{H}^0) = \hat{n}_b \left(\frac{\gamma_b m_b \beta_b^2 c^2}{2\pi \hat{T}_{\perp b}} \right) U \left(\frac{\gamma_b m_b \beta_b^2 c^2}{\hat{T}_{\perp b}} \mathcal{H}^0 \right). \tag{117}$$

Here, $\hat{n}_b$ and $\hat{T}_{\perp b}$ are positive constants with dimensions of density and temperature (energy units), respectively, $\mathcal{H}^0 = (1/2)(\tilde{X}'^2 + \tilde{Y}'^2) + (1/2)\kappa_f \tilde{R}^2 + \psi^0(\tilde{R})$ is the (dimensionless) Hamiltonian defined in Eq. (92), and $U(x)$ is the unit step function defined by $U(x) = 1$ for $0 \le x < 1$ and $U(x) = 0$ for $x > 1$. We take the on-axis self-field potential to be $\psi^0(\tilde{R} = 0) = 0$ and identify $\hat{n}_b = n_b^0(\tilde{R} = 0)$ with the on-axis beam density. For each choice of $F_b^0(\mathcal{H}^0)$ in Eqs. (115)–(117), the self-field potential $\psi^0(\tilde{R})$ is determined self-consistently in terms of the beam density $n_b^0(\tilde{R}) = \int d\tilde{X}' \, d\tilde{Y}' \, F_b^0(\mathcal{H}^0)$ from Eq. (95). Finally, for the general class of beam equilibria, $F_b^0(\mathcal{H}^0)$, the transverse temperature profile $T_{\perp b}^0(\tilde{R})$ is defined by Eq. (98).

A detailed evaluation of beam equilibrium properties for the choices of distribution functions in Eqs. (115)–(117) is presented elsewhere [21], and essential results are summarized in Table II. For each example, the inequality $\kappa_f \beta_b^2 c^2 > \hat{\omega}_{pb}^2 / 2\gamma_b^2$ is required to assure radial confinement of the beam particles, where $\hat{\omega}_{pb}^2 = 4\pi Z_b^2 e^2 \hat{n}_b / \gamma_b m_b$ is the on-axis plasma frequency squared. Moreover, in each case, the rms beam radius R_{b0} and unnormalized beam emittance ϵ_0 defined in Eq. (101) are related by the global force balance constraint in Eq. (107), and the unnormalized emittance ϵ_0 can be expressed as the average over perpendicular pressure given in Eq. (103).

It is evident from Table II that the equilibrium profiles for the density $n_b^0(\tilde{R})$ and perpendicular temperature $T_{\perp b}^0(\tilde{R})$ differ significantly for the three choices of equilibrium distribution functions in Eqs. (115)–(117). First, for the choice of thermal equilibrium distribution in Eq. (115), we note from Table II that the equilibrium density profile exhibits a highly nonlinear dependence on the self-field potential $\psi^0(\tilde{R})$, which must generally be determined by numerical integration of Eq. (95). The corresponding density profile, $n_b^0(\tilde{R}) = \hat{n}_b \exp\{-(\gamma_b m_b \beta_b^2 c^2 / 2\hat{T}_{\perp b})[\kappa_f \tilde{R}^2 + 2\psi^0(\tilde{R})]\}$, is generally bell shaped and radially diffuse, assuming a maximum value $(\hat{n}_b)$ at $\tilde{R} = 0$, and decreasing monotonically to zero

TABLE II. Equilibrium properties for various choices of $F_b^0(\mathcal{H}^0)$.

Distribution function $F_b^0(\mathcal{H}^0)$	Density profile $n_b^0(\tilde{R})$	Temperature profile $T_{\perp b}^0(\tilde{R})$	Transverse emittance ϵ_0^2
1. Thermal equilibrium in Eq. (115)	$\hat{n}_b \exp\{-\frac{\gamma_b m_b \beta_b^2 c^2}{2\hat{T}_{\perp b}}[\kappa_f \tilde{R}^2 + 2\psi^0]\}$	$\hat{T}_{\perp b} = \text{const}$	$\frac{8\hat{T}_{\perp b}}{\gamma_b m_b \beta_b^2 c^2} R_{b0}^2$
2. KV distribution in Eq. (116)	$\hat{n}_b = \text{const}$ for $0 \le \tilde{R} < r_{b0} \equiv \sqrt{2} R_{b0}$; (zero, otherwise)	$\hat{T}_{\perp b}(1 - \frac{\tilde{R}^2}{r_{b0}^2})$ for $0 \le \tilde{R} < r_{b0} \equiv \sqrt{2} R_{b0}$; (zero, otherwise)	$\frac{4\hat{T}_{\perp b}}{\gamma_b m_b \beta_b^2 c^2} R_{b0}^2$
3. Waterbag distribution in Eq. (117)	$\frac{I_0(r_{b0}/\lambda_D) - I_0(\tilde{R}/\lambda_D)}{I_0(r_{b0}/\lambda_D) - 1}$ for $0 \le \tilde{R} < r_{b0}$; (zero, otherwise)	$\hat{T}_{\perp b} \frac{n_b^0(\tilde{R})}{\hat{n}_b}$	Determined from Eq. (103)

with $n_b^0(\tilde{R} \to \infty) = 0$. At sufficiently low beam intensity with $\hat{\omega}_{pb}^2/2\gamma_b^2 \ll \kappa_f \beta_b^2 c^2$, it is found that the density profile is approximately Gaussian, with $n_b^0(\tilde{R}) \simeq \hat{n}_b \exp\{-\gamma_b m_b \beta_b^2 c^2 \kappa_f \tilde{R}^2/2\hat{T}_{\perp b}\}$. On the other hand, at very high beam intensity with $(\kappa_f \beta_b^2 c^2 - \hat{\omega}_{pb}^2/2\gamma_b^2)/\kappa_f \beta_b^2 c^2 = \delta \ll 1$, the density profile evaluated numerically from Table II and Eq. (95) is found to be radially very broad [21] in units of the thermal Debye length; i.e., $R_{b0} \gg \lambda_D \equiv (\gamma_b^2 \hat{T}_{\perp b}/4\pi \hat{n}_b Z_b^2 e^2)^{1/2}$. In this case, the density is approximately constant in the beam interior with $n_b^0(\tilde{R}) \simeq \hat{n}_b = \text{const}$, and $n_b^0(\tilde{R})$ drops rapidly to exponentially small values over a few Debye lengths at the beam surface. For the choice of equilibrium distribution function in Eq. (115), it also follows that the transverse temperature profile is uniform over the beam cross section, with $T_{\perp b}(\tilde{R}) = \hat{T}_{\perp b} = \text{const}$. Moreover, because $\partial F_b^0(\mathcal{H}^0)/\partial \mathcal{H}^0 \leq 0$ for the choice of distribution function in Eq. (115), it follows from Eq. (114) that the equilibrium is *stable* [25,26].

By contrast, at any beam intensity, the choice of (monoenergetic) equilibrium distribution function in Eq. (116) gives a *step-function* density profile, with $n_b^0(\tilde{R}) = \hat{n}_b = \text{const}$ for $0 \leq \tilde{R} < r_{b0} = \sqrt{2} R_{b0}$, and $n_b^0(\tilde{R}) = 0$ for $\tilde{R} > r_{b0}$. In this case, the beam has a "sharp" outer boundary at radius r_{b0} determined self-consistently from $(1/2)\kappa_f r_{b0}^2 + \psi^0(r_{b0}) = \hat{T}_{\perp b}/\gamma_b m_b \beta_b^2 c^2$, which gives $r_{b0}^2 = (2\hat{T}_{\perp b}/\gamma_b m_b)(\kappa_f \beta_b^2 c^2 - \hat{\omega}_{pb}^2/2\gamma_b^2)^{-1}$. Moreover, from Table II, unlike the thermal equilibrium case, the transverse temperature profile is parabolic, with $T_{\perp b}^0(\tilde{R}) = \hat{T}_{\perp b}(1 - \tilde{R}^2/r_{b0}^2)$ in the beam interior $(0 \leq \tilde{R} < r_{b0})$. Finally, a most important feature of Eq. (116) is that $F_b^0(\mathcal{H}^0)$ has a highly inverted population in energy, which is (singularly) peaked at $\mathcal{H}^0 = \hat{T}_{\perp b}/\gamma_b m_b \beta_b^2 c^2$. Therefore, as expected, there is free energy available to drive collective instabilities [10–14] for the choice of equilibrium distribution function in Eq. (116), at least at sufficiently high beam intensity.

Finally, from Table II, the choice of waterbag equilibrium distribution [16,17,21] in Eq. (117) also gives a density profile $n_b^0(\tilde{R})$ with sharp outer boundary at radius r_{b0}. In this case, r_{b0} is determined self-consistently from $I_0(r_{b0}/\lambda_D) = \kappa_f \beta_b^2 c^2/(\kappa_f \beta_b^2 c^2 - \hat{\omega}_{pb}^2/2\gamma_b^2)$, where $I_0(x)$ is the modified Bessel function of the first kind of order zero, and $\lambda_D = (\gamma_b^2 \hat{T}_{\perp b}/4\pi \hat{n}_b Z_b^2 e^2)^{1/2}$ is the thermal Debye length. Unlike the KV beam equilibrium, however, we note from Table II that the density profile $n_b^0(\tilde{R})$ decreases monotonically from the value $\hat{n}_b$ at $\tilde{R} = 0$ to zero at $\tilde{R} = r_{b0}$. Moreover, the transverse temperature profile has exactly the same radial shape as the density profile, with $T_{\perp b}^0(\tilde{R}) = (\hat{T}_{\perp b}/\hat{n}_b) n_b^0(\tilde{R})$. Similar to the case of a thermal equilibrium beam, the distribution function in Eq. (117) satisfies $\partial F_b^0(\mathcal{H}^0)/\partial \mathcal{H}^0 \leq 0$, and the waterbag equilibrium is expected to be stable [25,26] by virtue of Eq. (114).

C. Linearized Vlasov-Maxwell equations in the transformed variables

For completeness, and for application in future calculations of detailed stability properties, we summarize here the linearized Vlasov-Maxwell equations in the transformed variables $(\tilde{X}, \tilde{Y}, \tilde{X}', \tilde{Y}')$, assuming small-amplitude perturbations about the equilibrium distribution function $F_b^0(\mathcal{H}^0)$ and self-field potential $\psi^0(\tilde{R})$. In particular, we express $F_b(\tilde{X}, \tilde{Y}, \tilde{X}', \tilde{Y}', s) = F_b^0(\mathcal{H}^0) + \delta F_b(\tilde{X}, \tilde{Y}, \tilde{X}', \tilde{Y}', s)$ and $\psi(\tilde{X}, \tilde{Y}, s) = \psi^0(\tilde{R}) + \delta\psi(\tilde{X}, \tilde{Y}, s)$ in the Vlasov-Maxwell equations (83) and (84). In the linearization approximation, Eqs. (83) and (84) reduce to

$$\left\{\frac{\partial}{\partial t} + \tilde{X}' \frac{\partial}{\partial \tilde{X}} + \tilde{Y}' \frac{\partial}{\partial \tilde{Y}} - \left(\kappa_f \tilde{X} + \frac{\tilde{X}}{\tilde{R}} \frac{\partial \psi^0}{\partial \tilde{R}}\right) \frac{\partial}{\partial \tilde{X}'} - \left(\kappa_f \tilde{Y} + \frac{\tilde{Y}}{\tilde{R}} \frac{\partial \psi^0}{\partial \tilde{R}}\right) \frac{\partial}{\partial \tilde{Y}'}\right\} \delta F_b(\tilde{X}, \tilde{Y}, \tilde{X}', \tilde{Y}', s)$$
$$= \left[\left(\tilde{X}' \frac{\partial}{\partial \tilde{X}} + \tilde{Y}' \frac{\partial}{\partial \tilde{Y}}\right) \delta\psi(\tilde{X}, \tilde{Y}, s)\right] \frac{\partial}{\partial \mathcal{H}^0} F_b^0(\mathcal{H}^0), \quad (118)$$

and

$$\left(\frac{\partial^2}{\partial \tilde{X}^2} + \frac{\partial^2}{\partial \tilde{Y}^2}\right) \delta\psi(\tilde{X}, \tilde{Y}, s) = -\frac{2\pi K_b}{N_b} \int d\tilde{X}' \, d\tilde{Y}' \, \delta F_b(\tilde{X}, \tilde{Y}, \tilde{X}', \tilde{Y}', s). \quad (119)$$

Here, use has been made of Eq. (92) and the chain rule for differentiation to express $\partial F_b^0(\mathcal{H}^0)/\partial \tilde{X}' = \tilde{X}' \partial F_b^0(\mathcal{H}^0)/\partial \mathcal{H}^0$, etc. Because $\kappa_f = \text{const}$, a detailed stability analysis [12,21] based on Eqs. (118) and (119) in the transformed variables is greatly simplified in comparison with a stability analysis based on a linearization of Eqs. (3) and (4) in laboratory-frame variables. Furthermore, as noted earlier, a sufficient condition for stability [25,26] in the transformed variables is that the equilibrium distribution $F_b^0(\mathcal{H}^0)$ be a monotonically decreasing function of energy $\mathcal{H}^0$; i.e., $\partial F_b^0(\mathcal{H}^0)/\partial \mathcal{H}^0 \leq 0$ in Eq. (114). Whenever the inequality in Eq. (114) is satisfied, the perturbations δF_b and $\delta\psi$ solving Eqs. (118) and (119) do *not* grow exponentially. Equations (118) and (119), of course, can be used to determine detailed stability properties [12] for a wide variety of choices of equilibrium distribution function $F_b^0(\mathcal{H}^0)$.

V. PERIODICALLY FOCUSED BEAM PROPERTIES IN THE LABORATORY FRAME

As discussed in Sec. IV, in the slow variables $(\tilde{X}, \tilde{Y}, \tilde{X}', \tilde{Y}')$, a wide variety of equilibrium and stability properties can be calculated in a straightforward manner because the focusing force is constant ($\kappa_f = \text{const}$) in the transformed variables, and the simplest class of equilibrium distribution functions, $F_b^0(\mathcal{H}^0)$, correspond to beams with circular cross section. When transformed back to the laboratory frame, however, the beam is periodically focused, and its properties are generally s dependent. In this section, we carry out the back-transformation to the laboratory frame and calculate several properties of the beam, such as (a) the distribution function $f_b(x, y, x', y', s)$ (Sec. V A), (b) statistical averages such as the mean-square transverse beam dimensions, $\langle x^2 \rangle (s)$ and $\langle y^2 \rangle (s)$, and the unnormalized emittances, $\epsilon_x(s)$ and $\epsilon_y(s)$ (Sec. V B), and (c) macroscopic properties of the beam in the laboratory frame, such as the density profile $n_b(x, y, s)$ (Sec. V C). Throughout Sec. V, extensive use will be made of the inverse coordinate transformation, $\tilde{X}(x, y, x', y', s)$, $\tilde{Y}(x, y, x', y', s)$, etc., defined correct to order ϵ^3 in the Appendix [Eqs. (A1) and (A2) for a periodic-focusing quadrupole field and Eqs. (A3) and (A4) for a periodic-focusing solenoidal field]. In calculating the statistical averages in Sec. V B, we will also make use of the forward coordinate transformation, $x(\tilde{X}, \tilde{Y}, \tilde{X}', \tilde{Y}', s)$, $y(\tilde{X}, \tilde{Y}, \tilde{X}', \tilde{Y}', s)$, etc., defined correct to order ϵ^3 in Eqs. (87)–(90). In this regard, it is important to keep in mind the relative ordering of the various terms in Eqs. (87)–(90) and Eqs. (A1)–(A4). For example, $\alpha_q(s)$ and $\langle \alpha_q \rangle$ are of order ϵ, $\beta_q(s)$ is of order ϵ^2, etc. [see Eq. (91)].

A. Laboratory-frame distribution function $f_b(x, y, x', y', s)$

Once the distribution function $F_b(\tilde{X}, \tilde{Y}, \tilde{X}', \tilde{Y}', s)$ in the slow variables is calculated from Eqs. (83) and (84), it is straightforward to determine the corresponding distribution function $f_b(x, y, x', y', s)$ in the laboratory frame. Specifically, we make use of $f_b(x, y, x', y', s) \times dxdydx'dy' = F_b(\tilde{X}, \tilde{Y}, \tilde{X}', \tilde{Y}', s) d\tilde{X} d\tilde{Y} d\tilde{X}' d\tilde{Y}'$ [Eq. (85)] and the fact that the Jacobian of the (canonical) transformation is equal to unity [Eq. (86)] to obtain

$$f_b(x, y, x', y', s) = F_b\big(\tilde{X}(x, y, x', y', s), \tilde{Y}(x, y, x', y', s), \tilde{X}'(x, y, x', y', s), \tilde{Y}'(x, y, x', y', s), s\big). \tag{120}$$

In Eq. (120), the coordinate transformation $\tilde{X}(x, y, x', y', s)$, $\tilde{Y}(x, y, x', y', s)$, etc., is defined correct to order ϵ^3 in Eqs. (A1) and (A2) for a periodic-focusing quadrupole field and in Eqs. (A3) and (A4) for a periodic-focusing solenoidal field. In the important case where $F_b(\tilde{X}, \tilde{Y}, \tilde{X}', \tilde{Y}', s)$ corresponds to an *equilibrium* distribution $F_b^0(\mathcal{H}^0)$ in the transformed variables (see Sec. IV B), then the periodically focused distribution function in the laboratory frame is given by

$$f_b(x, y, x', y', s) = F_b^0[\mathcal{H}^0\big(\tilde{X}(x, y, x', y', s), \tilde{Y}(x, y, x', y', s), \tilde{X}'(x, y, x', y', s), \tilde{Y}'(x, y, x', y', s)\big)], \tag{121}$$

where $\mathcal{H}^0$ is defined by

$$\begin{aligned}\mathcal{H}^0&\big(\tilde{X}(x, y, x', y', s), \tilde{Y}(x, y, x', y', s), \tilde{X}'(x, y, x', y', s), \tilde{X}'(x, y, x', y', s)\big) \\ &= \frac{1}{2}[\tilde{X}'^2(x, y, x', y', s) + \tilde{Y}'^2(x, y, x', y', s)] + \frac{1}{2}\kappa_f \tilde{R}^2(x, y, x', y', s) + \psi^0\big(\tilde{R}(x, y, x', y', s)\big).\end{aligned} \tag{122}$$

Here, use has been made of Eq. (92), and $\tilde{R}(x, y, x', y', s)$ is defined by $\tilde{R}^2(x, y, x', y', s) = \tilde{X}^2(x, y, x', y', s) + \tilde{Y}^2(x, y, x', y', s)$. Because the s-dependent coefficients $\alpha_j(s)$, $\beta_j(s)$, etc., occurring in the orbit equations (A1)–(A4) have axial periodicity length $S = \text{const}$, it follows that the laboratory-frame distribution function defined in Eq. (121) also satisfies

$$f(x, y, x', y', s + S) = f(x, y, x', y', s). \tag{123}$$

Therefore, Eqs. (121) and (122) together with the coordinate transformations in Eqs. (A1)–(A4), map the equilibrium distribution function $F_b^0(\mathcal{H}^0)$, which is uniformly focused and has circular cross section in the transformed variables, into a pulsating, periodically focused distribution function in the laboratory frame.

The result in Eq. (121), together with the associated definitions in Eq. (122) and the Appendix, make accessible for the first time a broad class of high-intensity, periodically focused distribution functions that are analytically tractable, in addition to the familiar Kapchinskij-Vladimirskij equilibrium. Therefore, it is anticipated that Eq. (121) together with the results in Sec. IV B will be very useful in providing input data for numerical simulation studies based on the nonlinear Vlasov-Maxwell equations, as well as experimental studies of beam matching into periodic-focusing channels.

B. Statistical averages in the laboratory frame

From Eq. (12), the statistical average of a phase function $\chi(x, y, x', y', s)$ over the laboratory-frame distribution function $f_b(x, y, x', y', s)$ is defined by $\langle \chi \rangle (s) = N_b^{-1} \int dx\, dy\, dx'\, dy'\, \chi(x, y, x', y', s) f_b(x, y, x', y', s)$. For specified χ, the expressions for $f(x, y, x', y', s)$ in Eq. (120) or Eq. (121) can be used for a direct calculation of $\langle\chi\rangle(s)\cdots$. As an alternative (and simpler) approach we make use of the identity, $f_b(x,y,x',y',s)dxdydx'dy' = F(\tilde{X},\tilde{Y},\tilde{X}',\tilde{Y}',s)d\tilde{X}d\tilde{Y}d\tilde{X}'d\tilde{Y}'$, in Eq. (85) to express $\langle\chi\rangle(s)$ in the equivalent form

$$\langle\chi\rangle(s) = \int d\tilde{X}\,d\tilde{Y}\,d\tilde{X}'\,d\tilde{Y}'\,F_b(\tilde{X},\tilde{Y},\tilde{X}',\tilde{Y}',s) \times \chi\big(x(\tilde{X},\tilde{Y},\tilde{X}',\tilde{Y}',s), y(\tilde{X},\tilde{Y},\tilde{X}',\tilde{Y}',s), x'(\tilde{X},\tilde{Y},\tilde{X}',\tilde{Y}',s), y'(\tilde{X},\tilde{Y},\tilde{X}',\tilde{Y}',s), s\big)\,. \tag{124}$$

Here, the forward coordinate transformation, $x(\tilde{X},\tilde{Y},\tilde{X}',\tilde{Y}',s), y(\tilde{X},\tilde{Y},\tilde{X}',\tilde{Y}',s)$, etc., is defined correct to order ϵ^3 in Eqs. (87) and (88) for a periodic-focusing quadrupole field and in Eqs. (89) and (90) for a periodic-focusing solenoidal field. For the case where $F_b(\tilde{X},\tilde{Y},\tilde{X}',\tilde{Y}',s)$ corresponds to the class of self-consistent Vlasov equilibria, $F_b^0(\mathcal{H}^0)$, considered in Sec. IV, the statistical average defined in Eq. (124) further reduces to

$$\langle\chi\rangle(s) = \int d\tilde{X}\,d\tilde{Y}\,d\tilde{X}'\,d\tilde{Y}'\,F_b^0(\mathcal{H}^0) \times \chi\big(x(\tilde{X},\tilde{Y},\tilde{X}',\tilde{Y}',s), y(\tilde{X},\tilde{Y},\tilde{X}',\tilde{Y}',s), x'(\tilde{X},\tilde{Y},\tilde{X}',\tilde{Y}',s), y'(\tilde{X},\tilde{Y},\tilde{X}',\tilde{Y}',s), s\big)\,. \tag{125}$$

Given the relatively simple dependence of the coordinate transformations in Eqs. (87)–(90) on $(\tilde{X},\tilde{Y},\tilde{X}',\tilde{Y}')$, Eq. (125) provides a very straightforward prescription for evaluating statistical averages such as $\langle x^2\rangle(s)$, $\langle y^2\rangle(s)$, $\langle x'^2\rangle(s)$, etc., in the laboratory frame.

1. Periodic focusing quadrupole field

To illustrate the application of Eq. (125) to a periodic-focusing quadrupole field, we make use of Eqs. (87) and (125) to evaluate $\langle x^2\rangle(s)$. This readily gives $\langle x^2\rangle(s) = [1-\beta_q(s)]^2\langle\tilde{X}^2\rangle_0 + 4[\int_0^s ds\,\beta_q(s)]^2\langle\tilde{X}'^2\rangle_0 + 4[1-\beta_q(s)][\int_0^s ds\,\beta_q(s)]\langle\tilde{X}\tilde{X}'\rangle_0$, where $\langle\cdots\rangle$ denotes the statistical average over $F_b^0(\mathcal{H}^0)$ as defined in Eq. (99). Because $\langle\tilde{X}\tilde{X}'\rangle_0 = 0 = \langle\tilde{Y}\tilde{Y}'\rangle_0$ [Eq. (100)] and because $[\int_0^s ds\,\beta_q(s)]^2$ is of order ϵ^6 [Eq. (91)], we obtain

$$\begin{aligned}\langle x^2\rangle(s) &= [1-\beta_q(s)]^2\langle\tilde{X}^2\rangle_0\,,\\ \langle y^2\rangle(s) &= [1+\beta_q(s)]^2\langle\tilde{Y}^2\rangle_0\,,\end{aligned} \tag{126}$$

correct to order ϵ^3. Here, $\langle\tilde{X}^2\rangle_0 = \langle\tilde{Y}^2\rangle_0 = R_{b0}^2/2$ follows from Eq. (102). Defining $a^2(s) = [1-\beta_q(s)]^2R_{b0}^2 \simeq [1-2\beta_q(s)]R_{b0}^2$ and $b^2(s) = [1+\beta_q(s)]^2R_{b0}^2 \simeq [1+2\beta_q(s)]R_{b0}^2$, it follows from Eq. (126) that

$$\frac{\langle x^2\rangle}{a^2(s)} + \frac{\langle y^2\rangle}{b^2(s)} = 1\,. \tag{127}$$

We conclude from Eqs. (126) and (127) that the beam cross section in the laboratory frame corresponds to a pulsating ellipse (in an rms sense) with minor axes, $a(s)$ and $b(s)$. It should also be kept in mind that Eqs. (126) and (127) apply to the entire class of equilibrium distributions, $F_b^0(\mathcal{H}^0)$, in the transformed variables, and that self-field effects are allowed to be arbitrarily intense, consistent with radial confinement of the beam particles by the focusing field [Eq. (110)].

Other statistical averages of practical interest are also readily calculated from Eqs. (87), (88), and (125). Without presenting algebraic details, it is straightforward to show that

$$\begin{aligned}\langle x\rangle &= 0 = \langle y\rangle\,,\\ \langle x'\rangle &= 0 = \langle y'\rangle\,,\\ \langle x'^2\rangle(s) &= [1-\beta_q(s)]^2\langle\tilde{X}'^2\rangle_0 + [\alpha_q(s)-\langle\alpha_q\rangle]^2\langle\tilde{X}^2\rangle_0\,,\\ \langle y'^2\rangle(s) &= [1+\beta_q(s)]^2\langle\tilde{Y}'^2\rangle_0 + [\alpha_q(s)-\langle\alpha_q\rangle]^2\langle\tilde{Y}^2\rangle_0\,,\\ \langle xx'\rangle^2 &= [\alpha_q(s)-\langle\alpha_q\rangle]^2\langle\tilde{X}^2\rangle_0^2\,,\\ \langle yy'\rangle^2 &= [\alpha_q(s)-\langle\alpha_q\rangle]^2\langle\tilde{Y}^2\rangle_0^2\,,\end{aligned} \tag{128}$$

correct to order ϵ^3. Here, use has been made of Eq. (100), and we have expressed $\tilde{X}\partial\psi^0(\tilde{R})/\partial\tilde{X} - \tilde{Y}\partial\psi^0(\tilde{R})/\partial\tilde{Y} = (\tilde{X}^2-\tilde{Y}^2)\tilde{R}^{-1}\partial\psi^0(\tilde{R})/\partial\tilde{R}$ in the orbits for $x'(\tilde{X},\tilde{Y},\tilde{X}',\tilde{Y}',s)$ and $y'(\tilde{X},\tilde{Y},\tilde{X}',\tilde{Y}',s)$ in Eq. (88). Moreover, from Eq. (102), keep in mind that $\langle\tilde{X}^2\rangle_0 = \langle\tilde{Y}^2\rangle_0 = R_{b0}^2/2$ and $\langle\tilde{X}'^2\rangle_0 = \langle\tilde{Y}'^2\rangle_0 = (1/2)\times\langle\tilde{X}'^2+\tilde{Y}'^2\rangle_0$.

Equations (126) and (128) can be used to calculate the transverse emittances in the laboratory frame, $\epsilon_x^2(s) = 4[\langle x^2\rangle\langle x'^2\rangle - \langle xx'\rangle^2]$ and $\epsilon_y^2(s) = 4[\langle y^2\rangle\langle y'^2\rangle - \langle yy'\rangle^2]$, defined in Eq. (14). Because $\beta_q(s)$ is of order ϵ^2 [Eq. (91)], we note that $1-\beta_q^2(s)\simeq 1$ correct to order ϵ^3. Therefore, from Eqs. (126) and (128) we readily obtain

$$\begin{aligned}\epsilon_x^2(s) &= 4\langle\tilde{X}^2\rangle_0\langle\tilde{X}'^2\rangle_0 = \epsilon_{x0}^2 = \text{const}\,,\\ \epsilon_y^2(s) &= 4\langle\tilde{Y}^2\rangle_0\langle\tilde{Y}'^2\rangle_0 = \epsilon_{y0}^2 = \text{const}\,,\end{aligned} \tag{129}$$

correct to order ϵ^3. Therefore, from Eq. (129), the transverse emittances, $\epsilon_x(s)$ and $\epsilon_y(s)$, are conserved quantities (independent of s) correct to ϵ^3. In summary, the expressions for the laboratory-frame statistical averages in Eqs. (126)–(129) represent very powerful results, particularly because they apply to the entire class of equilibrium distribution functions, $F_b^0(\mathcal{H}^0)$, and because they allow for arbitrary beam intensity.

It is important to recognize the implications and limitations of Eq. (129); that is, the transverse emittances, $\epsilon_x(s)$ and $\epsilon_y(s)$, are conserved quantities when the back-transformation to the laboratory frame is carried out. First, and very important, Eq. (129) pertains to the class of *equilibrium* distributions $F_b^0(\mathcal{H}^0)$, which correspond to matched, constant-radius beam equilibria in the transformed variables (Sec. IV B) and transform back to matched, periodically focused solutions with period S in the laboratory frame [Eqs. (121)–(123)], at least to order ϵ^3. That is, Eq. (129) pertains to the transverse emittances associated with periodically focused beam equilibria in the laboratory frame. Of course, if the system is perturbed about equilibrium, i.e., $F_b(\tilde{X}, \tilde{Y}, \tilde{X}', \tilde{Y}', s) = F_b^0(\mathcal{H}^0) + \delta F_b(\tilde{X}, \tilde{Y}, \tilde{X}', \tilde{Y}', s)$, then the perturbations evolve self-consistently according to Eqs. (83) and (84), and there will be a corresponding change in the *total* laboratory-frame transverse emittances $\epsilon_x(s)$ and $\epsilon_y(s)$ [see Eqs. (14) and (120)] associated with the changes in F_b and ψ. It is well known that such variations in the laboratory-frame emittances about equilibrium values can be sizable [2,5], particularly if the equilibrium distribution $F_b^0(\mathcal{H}^0)$ is unstable, and there is a significant redistribution of particles in phase space. Second, and also important, in the equilibrium case it is important to keep in mind that Eq. (129) is an approximate result obtained in the context of the asymptotic analysis in Secs. III and IV (correct to order ϵ^3), and there are undoubtedly corrections to Eq. (129) of order ϵ^4 or smaller. Finally, referring ahead to Sec. V C, there is an important comparison to be made with Sacherer's classic analysis [39] of periodically focused intense beam propagation. For the case of constant emittances, ϵ_x and ϵ_y, analysis of Sacherer's rms envelope equations [39] shows that beam density profiles with an oscillatory elliptical cross section constitute self-consistent periodically focused solutions for intense beam propagation through a periodic quadrupole lattice. In Sec. V C, for a periodic quadrupole lattice, we find that the laboratory-frame density profile $n_b(x, y, s)$ corresponding to the beam equilibrium $F_b^0(\mathcal{H}^0)$ indeed has an oscillatory elliptical cross section [Eq. (136)]. In addition, however, the asymptotic analysis presented here demonstrates that the transverse emittances are constant, at least to order ϵ^3.

2. Periodic focusing solenoidal field

We now summarize several key results for statistical averages in the laboratory frame for the case of a periodic-focusing solenoidal field. In this case, we make use of Eq. (125), together with the coordinate transformations for $x(\tilde{X}, \tilde{Y}, \tilde{X}', \tilde{Y}', s)$, $y(\tilde{X}, \tilde{Y}, \tilde{X}', \tilde{Y}', s)$, etc., defined in Eqs. (89) and (90). The high degree of symmetry in the x and y motions in the solenoidal focusing field is, of course, reflected in the statistical averages. Paralleling the analysis for the quadrupole focusing case, and making use of Eqs. (89), (125), and $\langle \tilde{X}\tilde{X}' \rangle_0 = 0 = \langle \tilde{Y}\tilde{Y}' \rangle_0$, we readily obtain

$$\begin{aligned} \langle x^2 \rangle (s) &= [1 - \beta_s(s)]^2 \langle \tilde{X}^2 \rangle_0 \,, \\ \langle y^2 \rangle (s) &= [1 - \beta_s(s)]^2 \langle \tilde{Y}^2 \rangle_0 \,, \end{aligned} \tag{130}$$

correct to order ϵ^3. Here, $\langle \tilde{X}^2 \rangle_0 = \langle \tilde{Y}^2 \rangle_0 = R_{b0}^2/2$ follows from Eq. (102). From Eq. (130), the mean-square radius, $r_b^2(s) = \langle x^2 + y^2 \rangle (s)$, in the laboratory frame is given by

$$r_b^2(s) = [1 - \beta_s(s)]^2 R_{b0}^2 \,. \tag{131}$$

Because $\beta_s(s)$ is of order ϵ^2 [Eq. (91)], we can also express $[1 - \beta_s(s)]^2 \simeq 1 - 2\beta_s(s)$ correct to order ϵ^3 in Eq. (131). From Eqs. (130) and (131), for a periodic-focusing solenoidal field, we conclude that the beam cross section is circular and that the rms beam radius $r_b(s)$ oscillates with periodicity length S.

Other statistical averages of practical interest are also readily calculated from Eqs. (89), (90), and (125). Without presenting details, some straightforward algebraic manipulation that makes use of Eq. (102) and $\tilde{X}\partial\psi^0(\tilde{R})/\partial\tilde{X} + \tilde{Y}\partial\psi^0(\tilde{R})/\partial\tilde{Y} = \tilde{R}\partial\psi^0(\tilde{R})/\partial\tilde{R}$ gives

$$\begin{aligned} \langle x \rangle &= 0 = \langle y \rangle \,, \\ \langle x' \rangle &= 0 = \langle y' \rangle \,, \\ \langle x'^2 + y'^2 \rangle (s) &= [1 + \beta_s(s)]^2 \langle \tilde{X}'^2 + \tilde{Y}'^2 \rangle_0 \\ &\quad + [\alpha_s(s) - \langle \alpha_s \rangle]^2 \langle \tilde{X}^2 + \tilde{Y}^2 \rangle_0 \,, \\ \langle xx' + yy' \rangle^2 (s) &= [\alpha_s(s) - \langle \alpha_s \rangle]^2 \langle \tilde{X}^2 + \tilde{Y}^2 \rangle_0^2 \,, \end{aligned} \tag{132}$$

correct to order ϵ^3. Equations (131) and (132) can be used to calculate the total transverse emittance in the laboratory frame, defined by $\epsilon^2(s) = 4[\langle x^2 + y^2 \rangle \langle x'^2 + y'^2 \rangle - \langle xx' + yy' \rangle^2]$. Because $\beta_s(s)$ is of order ϵ^2, we note that $1 - \beta_s^2(s) \simeq 1$ correct to order ϵ^3. Therefore, from Eqs. (131) and (132) we obtain

$$\epsilon^2(s) = 4\langle \tilde{X}^2 + \tilde{Y}^2 \rangle_0 \langle X'^2 + \tilde{Y}'^2 \rangle_0 = \epsilon_0^2 = \text{const} \,, \tag{133}$$

correct to order ϵ^3. Therefore, from Eq. (133), the transverse emittance $\epsilon(s)$ is a conserved quantity (independent of s) correct to order ϵ^3.

Similar to the quadrupole focusing case, the results summarized in Eqs. (130)–(133) have a wide range of applicability. In particular, the results apply to the entire class of equilibrium distribution functions $F_b^0(\mathcal{H}^0)$, and the self fields are allowed to have arbitrary intensity.

C. Macroscopic profiles in the laboratory frame

Equation (121), supplemented by the definition of $\mathcal{H}^0$ in Eq. (122), provides a closed expression for the laboratory-frame distribution function $f_b(x, y, x', y', s)$ in terms of the transformed distribution function $F_b(\tilde{X}, \tilde{Y}, \tilde{X}', \tilde{Y}', s)$ for the case where $F_b = F_b^0(\mathcal{H}^0)$ corresponds to an equilibrium distribution in the transformed variables. As such, Eqs. (121) and (122), supplemented by the orbit transformations for $\tilde{X}(x, y, x', y', s)$, $\tilde{Y}(x, y, x', y', s)$, etc., defined in Eqs. (A1)–(A4) can be used for a direct evaluation of a wide variety of macroscopic profiles in the laboratory frame, such as the beam density profile, $n_b(x,y,s) = \int dx'\,dy'\,f_b(x,y,x',y',s)$, the transverse flow velocity, $\mathbf{V}_b(x,y,s) = n_b^{-1}\beta_b c \int dx'\,dy'(x'\hat{\mathbf{e}}_x + y'\hat{\mathbf{e}}_y)f_b(x,y,x',y',s)$, etc.

1. Density profile $n_b(x,y,s)$

For our purposes here, we illustrate an alternative (and perhaps simpler) approach for calculating the density profile $n_b(x,y,s)$ in the laboratory frame. Specifically, we express the density profile as $n_b(x,y,s) = \int d\tilde{x}\,d\tilde{y}\,dx'\,dy'\,f_b(\tilde{x},\tilde{y},x',y',s)\delta(\tilde{x}-x)\delta(\tilde{y}-y)$ and make use of the identity $f_b(\tilde{x},\tilde{y},x',y',s)d\tilde{x}d\tilde{y}dx'dy' = F_b^0(\tilde{X},\tilde{Y},\tilde{X}',\tilde{Y}')d\tilde{X}d\tilde{Y}d\tilde{X}'d\tilde{Y}'$, which follows from Eq. (85). Here, $F_b^0(\tilde{X},\tilde{Y},\tilde{X}',\tilde{Y}') = F_b^0(\mathcal{H}^0)$ is the equilibrium distribution function in the transformed variables (see Sec. IV B). It follows that $n_b(x,y,s)$ can be expressed in the equivalent form

$$n_b(x,y,s) = \int d\tilde{X}\,d\tilde{Y}\,d\tilde{X}'\,d\tilde{Y}'\,F_b^0(\tilde{X},\tilde{Y},\tilde{X}',\tilde{Y}') \times \delta[\tilde{x}(\tilde{X},\tilde{Y},\tilde{X}',\tilde{Y}',s) - x] \times \delta[\tilde{y}(\tilde{X},\tilde{Y},\tilde{X}',\tilde{Y}',s) - y]. \quad (134)$$

In Eq. (134), the coordinate transformations for $\tilde{x}(\tilde{X},\tilde{Y},\tilde{X}',\tilde{Y}',s)$ and $\tilde{y}(\tilde{X},\tilde{Y},\tilde{X}',\tilde{Y}',s)$ are defined in Eq. (87) for a periodic-focusing quadrupole field and in Eqs. (89) and (90) for a periodic-focusing solenoidal field.

For a periodic-focusing quadrupole field, we obtain from Eq. (87)

$$\begin{aligned}\tilde{x}(\tilde{X},\tilde{Y},\tilde{X}',\tilde{Y}',s) - x &= [1-\beta_q(s)]\left\{\tilde{X} - \frac{x}{[1-\beta_q(s)]} + \frac{2[\int_0^s ds\,\beta_q(s)]}{[1-\beta_q(s)]}\tilde{X}'\right\},\\ \tilde{y}(\tilde{X},\tilde{Y},\tilde{X}',\tilde{Y}',s) - y &= [1+\beta_q(s)]\left\{\tilde{Y} - \frac{y}{[1+\beta_q(s)]} - \frac{2[\int_0^s ds\,\beta_q(s)]}{[1+\beta_q(s)]}\tilde{Y}'\right\},\end{aligned} \quad (135)$$

where $\beta_q(s)$ is of order ϵ^2, and $\int_0^s ds\,\beta_q(s)$ is of order ϵ^3. Therefore, in leading order, the delta functions in Eq. (134) select $\tilde{X} = x/[1-\beta_q(s)]$ and $\tilde{Y} = y/[1+\beta_q(s)]$. Moreover, $F_b^0(\tilde{X},\tilde{Y},\tilde{X}',\tilde{Y}') = F_b^0(\mathcal{H}^0)$ in Eq. (134), and $\mathcal{H}^0 = (1/2)(\tilde{X}'^2 + \tilde{Y}'^2) + (1/2)\kappa_f\tilde{R}^2 + \psi^0(\tilde{R})$ depends on $\tilde{X}$ and $\tilde{Y}$ exclusively through the effective radial variable $\tilde{R} = (\tilde{X}^2 + \tilde{Y}^2)^{1/2}$. Substituting Eq. (135) into Eq. (134) then gives to leading order

$$n_b(x,y,s) = \frac{1}{[1-\beta_q^2(s)]}n_b^0[\tilde{R}(x,y,s)]. \quad (136)$$

Here, $\tilde{R}(x,y,s)$ is defined by $\tilde{R}^2(x,y,s) \equiv x^2/[1-\beta_q(s)]^2 + y^2/[1+\beta_q(s)]^2$, and we can approximate the multiplying factor $1/[1-\beta_q^2(s)] \simeq 1$ in Eq. (136) correct to order ϵ^3. In Eq. (136), the functional form of $n_b^0(\tilde{R})$ corresponds to the equilibrium density profile calculated self-consistently from Eq. (95) in the transformed variables. As such, Eq. (136) is applicable to a broad range of choices of equilibrium distribution functions $F_b^0(\mathcal{H}^0)$.

For a periodic-focusing solenoidal field, the analysis proceeds in a completely analogous manner, making use of the coordinate transformations for $\tilde{x}(\tilde{X},\tilde{Y},\tilde{X}',\tilde{Y}',s)$ and $\tilde{y}(\tilde{X},\tilde{Y},\tilde{X}',\tilde{Y}',s)$ defined in Eq. (89). Without presenting algebraic details, we obtain to leading order

$$n_b(x,y,s) = \frac{1}{[1-\beta_s(s)]^2}n_b^0[\tilde{R}(x,y,s)], \quad (137)$$

where $\tilde{R}(x,y,s)$ is defined by $\tilde{R}^2(x,y,s) \equiv x^2/[1-\beta_s(s)]^2 + y^2/[1-\beta_s(s)]^2$ in the periodic solenoidal case.

As expected, the density contours in the laboratory frame have an elliptical cross section for a periodic-focusing quadrupole field [Eq. (136)] and a circular cross section for a periodic-focusing solenoidal field [Eq. (137)]. Moreover, in both cases, it can be shown from Eqs. (136) and (137) that the number of particles per unit axial length is conserved; i.e., $N_b = \int dx\,dy\,n_b(x,y,s) = 2\pi\int_0^\infty d\tilde{R}\,\tilde{R}n_b^0(\tilde{R}) = \text{const}$ (independent of s).

Equations (136) and (137) are particularly attractive representations of the density profile $n_b(x,y,s)$ because the s-dependent distortion of the profiles appears explicitly in the definitions of $\tilde{R}(x,y,s)$. It should be pointed out, however, for continuously varying profiles $n_b^0(\tilde{R})$, that Eqs. (136) and (137) can also be Taylor expanded locally about a radius $r = (x^2+y^2)^{1/2}$ in the laboratory frame, treating $\beta_q(s)$ and $\beta_s(s)$ as small parameters (of order ϵ^2). For example, in the periodic quadrupole case, $\tilde{R}(x,y,s) = [x^2/(1-\beta_q)^2 + y^2/(1+\beta_q)^2]^{1/2} \simeq r + \beta_q(s)(x^2-y^2)/r$ for small $\beta_q(s)$. The expression for $n_b(x,y,s)$ in Eq. (136) can then be approximated by

$$n_b(x,y,s) = n_b^0(r) + \beta_q(s)\frac{(x^2-y^2)}{r}\frac{\partial}{\partial r}n_b^0(r), \quad (138)$$

correct to order ϵ^3. Equation (138) shows quite naturally the quadrupole distortion of the density profile in the laboratory frame by the periodic-focusing quadrupole field. Similarly, in the periodic solenoidal case, $\tilde{R}(x,y,s) = [(x^2+y^2)/(1-\beta_s)^2]^{1/2} \simeq r + \beta_s(s)r$, and the expression for $n_b(x,y,s)$ in Eq. (137) can be approximated by

$$\begin{aligned}n_b(x,y,s) &= n_b^0(r) + \beta_s(s)\left[2n_b^0(r) + r\frac{\partial}{\partial r}n_b^0(r)\right]\\ &= n_b^0(r) + \frac{\beta_s(s)}{r}\frac{\partial}{\partial r}[r^2 n_b^0(r)],\end{aligned} \quad (139)$$

correct to order ϵ^3. The (pulsating) profile in Eq. (139) of course remains axisymmetric in the laboratory frame for the case of a periodic-focusing solenoidal field.

2. Self-field potential $\psi(x, y, s)$

The self-field potential $\psi(x, y, s)$ in the laboratory frame is determined self-consistently in terms of the density profile $n_b(x, y, s)$ by integrating the Maxwell equation (4). For the case of a periodic-focusing quadrupole field, the density profile has the form given in Eq. (136). We introduce the minor dimensions defined by $a^2(s) = [1 - \beta_q(s)]^2 R_{b0}^2$ and $b^2(s) = [1 + \beta_q(s)]^2 R_{b0}^2$ [see Eq. (127)], where $R_{b0}^2 = N_b^{-1} 2\pi \int_0^\infty d\tilde{R}\, \tilde{R}^3 n_b^0(\tilde{R}) =$ const is the mean-square radius associated with the equilibrium distribution $F_b^0(\mathcal{H}^0)$ in the transformed variables defined in Eq. (101). Substituting Eq. (136) into Eq. (4) then gives

$$\left(\frac{\partial^2}{\partial x^2} + \frac{\partial^2}{\partial y^2}\right)\psi(x, y, s) = -\frac{2\pi K_b}{N_b} \frac{R_{b0}^2}{a(s)b(s)} n_b^0\left[\frac{\tilde{R}(x, y, s)}{R_{b0}}\right], \tag{140}$$

where $\tilde{R}(x, y, s)/R_{b0}$ is defined by

$$\frac{\tilde{R}(x, y, s)}{R_{b0}} = \left[\frac{x^2}{a^2(s)} + \frac{y^2}{b^2(s)}\right]^{1/2}. \tag{141}$$

In Eq. (140), we have introduced the scaled radial variable $\tilde{R}(x, y, s)/R_{b0}$ in the argument of $n_b^0(\tilde{R}/R_{b0})$ without loss of generality. Taking ψ, $\partial\psi/\partial x$, and $\partial\psi/\partial y$ to be equal to zero at $(x, y) = (0, 0)$, the exact solutions to Eq. (140) for the self-field force components in the laboratory frame, $F_x^s = -\partial\psi/\partial x$ and $F_y^s = -\partial\psi/\partial y$, are given by [39]

$$\begin{aligned} -\frac{\partial}{\partial x}\psi(x, y, s) &= \frac{\pi K_b}{N_b} R_{b0}^2 x \int_0^\infty \frac{d\xi\, n_b^0[T(x, y, s, \xi)]}{[a^2(s) + \xi]^{3/2}[b^2(s) + \xi]^{1/2}}, \\ -\frac{\partial}{\partial y}\psi(x, y, s) &= \frac{\pi K_b}{N_b} R_{b0}^2 y \int_0^\infty \frac{d\xi\, n_b^0[T(x, y, s, \xi)]}{[a^2(s) + \xi]^{1/2}[b^2(s) + \xi]^{3/2}}, \end{aligned} \tag{142}$$

where $T(x, y, s, \xi)$ is defined by

$$T(x, y, s, \xi) = \left[\frac{x^2}{a^2(s) + \xi} + \frac{y^2}{b^2(s) + \xi}\right]^{1/2}. \tag{143}$$

For a specified functional form of $n_b^0(\tilde{R}/R_{b0})$, Eq. (142) can be used to calculate the detailed dependence of $-\partial\psi/\partial x$ and $-\partial\psi/\partial y$ on (x, y, s).

The transverse self-field force is even simpler to determine for the case of a periodic-focusing solenoidal field because of the azimuthal symmetry of $\psi(r, s)$ in the laboratory frame. In this case we introduce the mean-square radius $r_b^2(s) = [1 - \beta_s(s)]^2 R_{b0}^2$ defined in Eq. (131) and express $\tilde{R}(x, y, s)/R_{b0} = [(x^2 + y^2)/(1 - \beta_s)^2 R_{b0}^2]^{1/2} = r/r_b(s)$. Substituting Eq. (137) into the Maxwell equation (4) for $\psi(r, s)$ then gives

$$\frac{1}{r}\frac{\partial}{\partial r} r \frac{\partial}{\partial r}\psi(r, s) = -\frac{2\pi K_b}{N_b} \frac{R_{b0}^2}{r_b^2(s)} n_b^0\left[\frac{r}{r_b(s)}\right]. \tag{144}$$

Solving Eq. (144) for the radial self-field force, $F_r^s = -\partial\psi/\partial r$, then gives

$$-\frac{\partial}{\partial r}\psi(r, s) = \frac{2\pi K_b}{N_b} \frac{R_{b0}^2}{r} \int_0^{r/r_b(s)} dT\, T n_b^0(T). \tag{145}$$

Similar to the periodic quadrupole case, once the functional form of $n_b^0(\tilde{R})$ is determined self-consistently for a specified equilibrium distribution function, $F_b^0(\mathcal{H}^0)$, in the transformed variables, Eq. (145) can be used to determine the corresponding self-field force in the laboratory frame which is a periodic function of s.

3. Transverse flow velocity $\mathbf{V}_b(x, y, s)$

For a specified equilibrium distribution function, $F_b^0(\mathcal{H}^0)$, in the transformed variables, the corresponding laboratory-frame distribution function, $f_b(x, y, x', y', s)$, defined in Eq. (121) can be used to calculate other macroscopic properties, such as the transverse temperature profiles, flow velocity components, etc. We illustrate this with a direct calculation of the transverse flow velocity defined (in dimensional units) by

$$\mathbf{V}_b(x, y, s) = [n_b(x, y, s)]^{-1}\beta_b c \int dx'\, dy'[x'\hat{\mathbf{e}}_x + y'\hat{\mathbf{e}}_y] \times f_b(x, y, x', y', s). \tag{146}$$

For present purposes, we consider the case of a periodic-focusing solenoidal field, where the inverse coordinate transformation, $\tilde{X}(x, y, x', y', s)$, $\tilde{Y}(x, y, x', y', s)$, etc., occurring in the definition of $\mathcal{H}^0$ in Eq. (122) is defined in Eqs. (A3) and (A4). Of particular importance when calculating the velocity moments in Eq. (146) are the symmetries associated with the kinetic energy term, $(1/2)[\tilde{X}'^2(x, y, x', y', s) + \tilde{Y}'^2(x, y, x', y', s)]$, in Eq. (122). Making use of $x\partial\psi/\partial x + y\partial\psi/\partial y = r\partial\psi/\partial r$, we find from Eqs. (A3) and (A4) that

$$[\tilde{X}'^2(x,y,x',y',s) + \tilde{Y}'^2(x,y,x',y',s)] = \Bigg[[1-\beta_s(s)]x' - \Bigg\{ -[\alpha_s(s) - \langle\alpha_s\rangle][1+\beta_s(s)] - \left(\int_0^s ds[\delta_s(s) - \langle\delta_s\rangle]\right) + 2\bar{\kappa}_s\left[\int_0^s ds\,\beta_s(s)\right] - \left[\int_0^s ds\,\beta_s(s)\right]\frac{1}{r}\frac{\partial}{\partial r} r\frac{\partial\psi}{\partial r}\Bigg\} x\Bigg]^2 + \Bigg[[1-\beta_s(s)]y' - \Bigg\{ -[\alpha_s(s) - \langle\alpha_s\rangle][1+\beta_s(s)] - \left(\int_0^s ds[\delta_s(s) - \langle\delta_s\rangle]\right) + 2\bar{\kappa}_s\left[\int_0^s ds\,\beta_s(s)\right] - \left[\int_0^s ds\,\beta_s(s)\right]\frac{1}{r}\frac{\partial}{\partial r} r\frac{\partial\psi}{\partial r}\Bigg\} y\Bigg]^2 . \tag{147}$$

To calculate the transverse flow velocity defined in Eq. (146), we make use of Eqs. (121), (122), and (147), keeping in mind the relative size of the various terms in Eq. (147) [see Eq. (91)] and approximating (for example) $(1-\beta_s)x' - \{\cdots\}x = (1-\beta_s)[x' - \{\cdots\}x/(1-\beta_s)] \simeq (1-\beta_s)[x' - \{\cdots\}(1+\beta_s)x]$. Some straightforward algebra shows that the transverse flow velocity is purely radial with

$$\mathbf{V}_b(x,y,s) = V_{rb}(r,s)\hat{\mathbf{e}}_r , \tag{148}$$

where $V_{rb}(r,s)$ is defined by

$$V_{rb}(r,s) = \beta_b c\Bigg\{ [-\alpha_s(s) + \langle\alpha_s\rangle][1+2\beta_s(s)] - \left(\int_0^s ds[\delta_s(s) - \langle\delta_s\rangle]\right) + 2\bar{\kappa}_s\left[\int_0^s ds\,\beta_s(s)\right] - \left[\int_0^s ds\,\beta_s(s)\right]\frac{1}{r}\frac{\partial}{\partial r} r\frac{\partial\psi}{\partial r}\Bigg\} r , \tag{149}$$

correct to order ϵ^3. Here, $x\hat{\mathbf{e}}_x + y\hat{\mathbf{e}}_y = r\hat{\mathbf{e}}_r$, where $\hat{\mathbf{e}}_r = \cos\theta\hat{\mathbf{e}}_x + \sin\theta\hat{\mathbf{e}}_y$ is a unit vector in the radial direction, and we have neglected terms proportional to $\beta_s(s)[\int_0^s ds\,\beta_s(s)]$, which are of order ϵ^5.

The transverse flow velocity can be calculated in a similar manner for a periodic-focusing quadrupole field, although the flow pattern is more complicated than in Eq. (148) because of the elliptical cross section of the beam.

D. Range of validity of asymptotic expansion procedure

To conclude Sec. V, we summarize the illustrative conditions required for validity of the present asymptotic expansion procedure for the case of a periodic-focusing quadrupole lattice with the sinusoidal waveform considered in Table I. Here, the strength of the focusing field is measured by the dimensionless parameter $\lambda_q \equiv \hat{\kappa}_q S^2/2\pi$, and the characteristic vacuum phase advance is defined by $\sigma_{ov} = \sqrt{\kappa_{fq}}\,S$, where $\kappa_{fq} \equiv (3/2)\lambda_q^2/S^2$ [see Table I and Eq. (109)]. For this choice of focusing lattice, it follows that λ_q and σ_{ov} are related by

$$\frac{\lambda_q}{2\pi} = \sqrt{\frac{2}{3}}\,\frac{\sigma_{ov}}{2\pi} . \tag{150}$$

Therefore, $\lambda_q < (2/3)^{1/2} = 0.82$ corresponds to $\sigma_{ov} < 1$ (vacuum phase advance less than 60°). We now consider the relative size of the various terms in the coordinate transformation relating (x,y,x',y') to $(\tilde{X},\tilde{Y},\tilde{X}',\tilde{Y}')$ in Eqs. (87) and (88). Here, we estimate the characteristic (maximum) values by

$$|x| \sim |\tilde{X}| \sim |y| \sim |\tilde{Y}| \sim r_b ,$$
$$|x'| \sim |\tilde{X}'| \sim |y'| \sim |\tilde{Y}'| \sim r_b/S , \tag{151}$$
$$|\psi| \sim K_b ,$$

where r_b is the characteristic (rms) beam radius, K_b is the dimensionless self-field perveance defined in Eq. (5), and use has been made of Maxwell's equation (84) and $N_b \sim \pi r_b^2 n_b$ to estimate $|\psi| \sim K_b$. The correction terms to $x = \tilde{X}$ and $y = \tilde{Y}$ in Eq. (87) then stand in the ratio

$$|\beta_q| : \frac{|\int_0^s ds\,\beta_q|}{S} . \tag{152}$$

Similarly, the correction terms to $x' = \tilde{X}'$ and $y' = \tilde{Y}'$ in Eq. (88) stand in the ratio

$$|\beta_q| : S|\alpha_q| : S|\alpha_q\beta_q| : S\left|\int_0^s ds[\delta_q - \langle\delta_q\rangle]\right| : \frac{|\int_0^s ds\,\beta_q|}{S}\,\frac{S^2|\psi|}{r_b^2} , \tag{153}$$

where we have estimated $|\partial\psi/\partial\tilde{X}| \sim |\psi|/r_b$, etc.

We now make use of the entries in Table I and the estimate $|\psi| \sim K_b$ in Eq. (151) to compare the size of the various terms in Eqs. (152) and (153). We readily find that the correction terms in Eq. (152) stand in the ratio

$$\frac{\lambda_q}{2\pi} : \frac{2\lambda_q}{(2\pi)^2} . \tag{154}$$

Similarly, the correction terms in Eq. (153) stand in the ratio

$$\frac{\lambda_q}{2\pi} : \lambda_q : \frac{\lambda_q^2}{2\pi} : \frac{\lambda_q^2}{2\pi} : \frac{\lambda_q}{(2\pi)^2} \cdot \frac{S^2 K_b}{r_b^2} . \tag{155}$$

From Eq. (107), the *largest* value of the self-field perveance K_b allowed in the limit of negligibly small transverse emittance is $K_b \sim \kappa_{fq} r_b^2$, which gives $K_b S^2/r_b^2 \sim \kappa_{fq} S^2 = (3/2)\lambda_q^2$. Therefore, in the limit of intense space-charge field, the ratio of terms in Eq. (155) reduces to

$$\frac{\lambda_q}{2\pi} : \lambda_q : \frac{\lambda_q^2}{2\pi} : \frac{\lambda_q^2}{2\pi} : \frac{3}{2} \frac{\lambda_q^3}{(2\pi)^2} . \tag{156}$$

Therefore, from Eqs. (154) and (156), we conclude that the key small parameter required for validity of the present asymptotic analysis is $\epsilon = \lambda_q/2\pi < 1$, at least for the case of a sinusoidal quadrupole focusing field considered in Table I. From Eq. (150), this corresponds to $\sigma_{ov}/2\pi < (3/2)^{1/2}$, which leads to the conjecture (Sec. I) that the phase advance σ_0 should be smaller than $60° \, (= \pi/3)$. The important practical test of the range of validity awaits detailed comparison with experiment and numerical simulations.

VI. CONCLUSIONS

In this paper, we have developed and applied a third-order Hamiltonian averaging technique for investigating solutions to the nonlinear Vlasov-Maxwell equations for the case of an intense ion beam propagating through a periodic-focusing quadrupole field or a periodic-focusing solenoidal field. The formalism used a canonical transformation given by an expanded generating function to transform away the rapidly oscillating terms and end up with a Hamiltonian $\mathcal{H}$ that depends only on slow variables. The assumptions and theoretical model were summarized in Sec. II, including the nonlinear Vlasov-Maxwell equations for the distribution function $f_b(x, y, x', y', s)$ and self-field potential $\psi(x, y, s)$ in the laboratory frame. In Sec. III, we made use of Channell's third-order Hamiltonian averaging technique [34] to transform from laboratory-frame variables (x, y, x', y') to a new Hamiltonian $\mathcal{H}(\tilde{X}, \tilde{Y}, \tilde{X}', \tilde{Y}', s)$ in the slow variables $(\tilde{X}, \tilde{Y}, \tilde{X}', \tilde{Y}')$ correct to order ϵ^3. The formalism employed a canonical transformation given by an expanded generating function to transform away the rapidly oscillating terms. This led to a Hamiltonian $\mathcal{H}(\tilde{X}, \tilde{Y}, \tilde{X}', \tilde{Y}', s)$ in the transformed variables of the form given in Eq. (79), where $\kappa_f = \text{const}$. An important by-product of the generating function analysis was the determination of the coordinate transformation that relates the laboratory-frame variables (x, y, x', y') to the slow variables $(\tilde{X}, \tilde{Y}, \tilde{X}', \tilde{Y}')$ [Eqs. (87)–(90)]. The major simplification associated with transforming to the slow variables $(\tilde{X}, \tilde{Y}, \tilde{X}', \tilde{Y}')$ is immediately evident from the expression for $\mathcal{H}(\tilde{X}, \tilde{Y}, \tilde{X}', \tilde{Y}', s)$ in Eq. (79). In particular, the focusing coefficient κ_f is both *constant* (independent of s) and *isotropic* in the transverse plane. This should be contrasted with the expression in Eq. (6) for the Hamiltonian $\hat{H}(x, y, x', y', s)$ in the laboratory frame, where the focusing coefficients $\kappa_x(s)$ and $\kappa_y(s)$ are rapidly oscillating functions of s. In Sec. IV, following a discussion of the nonlinear Vlasov-Maxwell equations for $F_b(\tilde{X}, \tilde{Y}, \tilde{X}', \tilde{Y}', s)$ and $\psi(\tilde{X}, \tilde{Y}, s)$ in the transformed variables, we presented several examples of axisymmetric equilibrium solutions, i.e., distribution functions $F_b^0(\mathcal{H}^0)$ with $\partial/\partial s = 0$ and $\partial/\partial\Theta = 0$ corresponding to constant-radius beam equilibria with a circular cross section in the transformed variables [12,21]. Of particular note is the class of distribution functions that satisfy $\partial F_b^0(\mathcal{H}^0)/\partial H^0 \le 0$, which can be shown to be *stable* [25,26]. Finally, in Sec. V, we exploited the inverse coordinate transformation, $\tilde{X}(x, y, x', y', s)$, $\tilde{Y}(x, y, x', y', s)$, etc., to determine properties of the *periodically focused* distribution function $f_b(x, y, x', y', s)$ in the laboratory frame, correct to order ϵ^3, consistent with the class of constant-radius circular cross-section beam equilibria $F_b^0(\mathcal{H}^0)$ in the transformed variables. A wide range of important physical quantities were determined, including the distribution function $f_b(x, y, x', y', s)$; statistical averages such as the transverse mean-square beam dimensions, $\langle x^2 \rangle(s)$ and $\langle y^2 \rangle(s)$, and the unnormalized emittances, $\epsilon_x(s)$ and $\epsilon_y(s)$; and macroscopic properties such as the number density of beam particles, $n_b(x, y, s) = \int dx'\, dy'\, f_b(x, y, x', y', s)$, the self-field potential, $\psi(x, y, s)$, etc. Finally, in Sec. V D, we summarized the illustrative conditions required for validity of the present asymptotic expansion procedure for the case of a periodic-focusing quadrupole lattice with sinusoidal waveform (Table I). The important practical test awaits detailed comparison with experiment and numerical simulations.

ACKNOWLEDGMENTS

This research was supported by the Department of Energy and the Short Pulse Spallation Source Project and LANSCE Division of Los Alamos National Laboratory, and in part by the Office of Naval Research.

APPENDIX: INVERSE COORDINATE TRANSFORMATION

The coordinate transformations in Eqs. (87)–(90) relate the laboratory-frame coordinates $x(\tilde{X}, \tilde{Y}, \tilde{X}', \tilde{Y}', s)$, $y(\tilde{X}, \tilde{Y}, \tilde{X}', \tilde{Y}', s)$, etc., directly to the slow variables

$(\tilde{X}, \tilde{Y}, \tilde{X}', \tilde{Y}')$. The *inverse* transformations, which relate the slow coordinates $\tilde{X}(x, y, x', y', s)$, $\tilde{Y}(x, y, x', y', s)$, etc., to the laboratory-frame variables (x, y, x', y'), can be calculated from Eqs. (87)–(90) correct to order ϵ^3. In this regard, it is important to make use of the relative sizes of the various terms in Eqs. (87)–(90), which correspond to the orderings summarized in Eq. (91).

The procedure for calculating the inverse transformation is relatively straightforward. For example, for the case of a periodic-focusing quadrupole field it follows from Eq. (87) that $\tilde{X} = x/(1 - \beta_q) - 2[\int_0^s ds\, \beta_q(s)]\tilde{X}'$, which can be approximated by $\tilde{X} = (1 + \beta_q)x - 2[\int_0^s ds\, \beta_q(s)]x'$ correct to order ϵ^3, where use has been made of Eqs. (88) and (91). A similar expression for $\tilde{Y}$ in terms of y and y' can be obtained from Eqs. (87), (88), and (91), and Eq. (88) can also be solved for $\tilde{X}'$ and $\tilde{Y}'$ in terms of the laboratory-frame variables (x, y, x', y'). Without presenting algebraic details, for the case of a periodic-focusing quadrupole field, we obtain from Eqs. (87), (88), and (91) the inverse transformation

$$\begin{aligned}\tilde{X}(x, y, x', y', s) &= [1 + \beta_q(s)]x - 2\left[\int_0^s ds\, \beta_q(s)\right]x', \\ \tilde{Y}(x, y, x', y', s) &= [1 - \beta_q(s)]y + 2\left[\int_0^s ds\, \beta_q(s)\right]y',\end{aligned} \tag{A1}$$

and

$$\begin{aligned}\tilde{X}'(x, y, x', y', s) = [1 - \beta_q(s)]x' &- \left\{-[\alpha_q(s) - \langle\alpha_q\rangle][1 + \beta_q(s)] - \left(\int_0^s ds[\delta_q(s) - \langle\delta_q\rangle]\right)\right\}x \\ &- \left[\int_0^s ds\, \beta_q(s)\right]\frac{\partial}{\partial x}\left(x\frac{\partial\psi}{\partial x} - y\frac{\partial\psi}{\partial y}\right), \\ \tilde{Y}'(x, y, x', y', s) = [1 + \beta_q(s)]y' &- \left\{[\alpha_q(s) - \langle\alpha_q\rangle][1 - \beta_q(s)] - \left(\int_0^s ds[\delta_q(s) - \langle\delta_q\rangle]\right)\right\}y \\ &+ \left[\int_0^s ds\, \beta_q(s)\right]\frac{\partial}{\partial y}\left(y\frac{\partial\psi}{\partial y} - x\frac{\partial\psi}{\partial x}\right),\end{aligned} \tag{A2}$$

correct to order ϵ^3.

Similarly, for the case of a periodic-focusing solenoidal field, we obtain from Eqs. (89)–(91) the inverse transformation

$$\begin{aligned}\tilde{X}(x, y, x', y', s) &= [1 + \beta_s(s)]x - 2\left[\int_0^s ds\, \beta_s(s)\right]x', \\ \tilde{Y}(x, y, x', y', s) &= [1 + \beta_s(s)]y - 2\left[\int_0^s ds\, \beta_s(s)\right]y',\end{aligned} \tag{A3}$$

and

$$\begin{aligned}\tilde{X}'(x, y, x', y', s) = {} & [1 - \beta_s(s)]x' - \left\{-[\alpha_s(s) - \langle\alpha_s\rangle][1 + \beta_s(s)] - \left(\int_0^s ds[\delta_s(s) - \langle\delta_s\rangle]\right)\right. \\ & \left. + 2\bar{\kappa}_s\left[\int_0^s ds\, \beta_s(s)\right]\right\}x - \left[\int_0^s ds\, \beta_s(s)\right]\frac{\partial}{\partial x}\left(x\frac{\partial\psi}{\partial x} + y\frac{\partial\psi}{\partial y}\right), \\ \tilde{Y}'(x, y, x', y', s) = {} & [1 - \beta_s(s)]y' - \left\{-[\alpha_s(s) - \langle\alpha_s\rangle][1 + \beta_s(s)] - \left(\int_0^s ds[\delta_s(s) - \langle\delta_s\rangle]\right)\right. \\ & \left. + 2\bar{\kappa}_s\left[\int_0^s ds\, \beta_s(s)\right]\right\}y - \left[\int_0^s ds\, \beta_s(s)\right]\frac{\partial}{\partial y}\left(x\frac{\partial\psi}{\partial x} + y\frac{\partial\psi}{\partial y}\right),\end{aligned} \tag{A4}$$

correct to order ϵ^3.

In obtaining Eqs. (A1)–(A4), we have made use of the fact that the self-field contributions in Eqs. (88) and (90) are proportional to $\int_0^s ds\, \beta_q(s)$ and $\int_0^s ds\, \beta_s(s)$, respectively, which are of order ϵ^3 [see Eq. (91)]. Therefore, to leading order, we approximate $(\partial/\partial\tilde{X})(\tilde{X}\partial/\partial\tilde{X} - \tilde{Y}\partial/\partial\tilde{Y})\psi(\tilde{X}, \tilde{Y}, s)$ by $(\partial/\partial x)(x\partial/\partial x - y\partial/\partial y)\psi(x, y, s)$, etc., in obtaining the inverse transformations in Eqs. (A2) and (A4).

[1] R. C. Davidson, *Physics of Nonneutral Plasmas* (Addison-Wesley Publishing Co., Reading, MA, 1990), and references therein.
[2] T. P. Wangler, *Principles of RF Linear Accelerators* (Wiley, New York, 1998).
[3] J. D. Lawson, *The Physics of Charged-Particle Beams* (Oxford Science Publications, New York, 1988).
[4] D. A. Edwards and M. J. Syphers, *An Introduction to the Physics of High-Energy Accelerators* (Wiley, New York, 1993).
[5] M. Reiser, *Theory and Design of Charged Particle Beams* (Wiley, New York, 1994).
[6] R. A. Jameson, in *Advanced Accelerator Concepts*, edited by J. S. Wurtele, AIP Conf. Proc. No. 279 (AIP, New York, 1993), p. 969.
[7] E. P. Lee and J. Hovingh, Fusion Technol. **15**, 369 (1989).
[8] See, for example, *Proceedings of the 11th International Symposium on Heavy Ion Inertial Fusion*, edited by J. J. Barnard, T. J. Fessenden, and E. P. Lee [Fusion Eng. Des. **32**, 1–620 (1996)], and references therein.
[9] See, for example, *Proceedings of the 12th International Symposium on Heavy Ion Inertial Fusion*, edited by I. Hofmann [Nucl. Instrum. Methods Phys. Res., Sect. A **415**, 1–725 (1998)].
[10] I. Kapchinskij and V. Vladimirskij, in *Proceedings of the International Conference on High Energy Accelerators and Instrumentation* (CERN Scientific Information Service, Geneva, 1959), p. 274.
[11] R. L. Gluckstern, in *Proceedings of the 1970 Proton Linear Accelerator Conference, Batavia, IL*, edited by M. R. Tracy (National Accelerator Laboratory, Batavia, IL, 1971), p. 811.
[12] See, for example, *Physics of Nonneutral Plasmas* (Ref. [1]), Chaps. 2, 4, 9, and 10, and references therein.
[13] T. -S. Wang and L. Smith, Part. Accel. **12**, 247 (1982).
[14] I. Hofmann, L. J. Laslett, L. Smith, and I. Haber, Part. Accel. **13**, 145 (1983).
[15] J. Struckmeier and J. Klabunde, Part. Accel. **15**, 47 (1984).
[16] I. Hofmann and J. Struckmeier, Part. Accel. **21**, 69 (1987).
[17] J. Struckmeier and I. Hofmann, Part. Accel. **39**, 219 (1992).
[18] N. Brown and M. Reiser, Phys. Plasmas **2**, 965 (1995).
[19] R. L. Gluckstern, W.-H. Cheng, and H. Ye, Phys. Rev. Lett. **75**, 2835 (1995).
[20] C. Chen and R. C. Davidson, Phys. Rev. E **49**, 5679 (1994).
[21] R. C. Davidson and C. Chen, Part. Accel. **59**, 175 (1998).
[22] R. C. Davidson and C. Chen, Nucl. Instrum. Methods Phys. Res., Sect. A **415**, 370 (1998).
[23] C. Chen, R. Pakter, and R. C. Davidson, Phys. Rev. Lett. **79**, 225 (1997).
[24] R. C. Davidson, W. W. Lee, and P. H. Stoltz, Phys. Plasmas **5**, 279 (1998).
[25] R. C. Davidson, Phys. Rev. Lett. **81**, 991 (1998).
[26] R. C. Davidson, Phys. Plasmas **5**, 3459 (1998).
[27] P. H. Stoltz, R. C. Davidson, and W. W. Lee, Phys. Plasmas **6**, 298 (1999).
[28] P. H. Stoltz, W. W. Lee, and R. C. Davidson, Nucl. Instrum. Methods Phys. Res., Sect. A **415**, 433 (1998).
[29] W. W. Lee, Q. Qian, and R. C. Davidson, Phys. Lett. A **230**, 347 (1997).
[30] Q. Qian, W. W. Lee, and R. C. Davidson, Phys. Plasmas **4**, 1915 (1997).
[31] A. Friedman and D. P. Grote, Phys. Fluids B **4**, 2203 (1992).
[32] A. Friedman, J. J. Barnard, D. P. Grote, and I. Haber, Nucl. Instrum. Methods Phys. Res., Sect. A **415**, 455 (1998).
[33] S. M. Lund, J. J. Barnard, G. D. Craig, A. Friedman, D. P. Grote, H. S. Hopkins, T. S. Sangster, W. M. Sharp, S. Eylon, T. T. Fessenden, E. Henestroza, S. Yu, and I. Haber, Nucl. Instrum. Methods Phys. Res., Sect. A **415**, 345 (1998).
[34] P. J. Channell, Phys. Plasmas **6**, 982 (1999).
[35] H. Goldstein, *Classical Mechanics* (Addison-Wesley, Reading, MA, 1980), 2nd ed.
[36] L. D. Landau and E. M. Lifshitz, *Classical Mechanics* (Pergamon, New York, 1991).
[37] V. I. Arnold, *Mathematical Methods of Classical Mechanics* (Springer-Verlag, New York, 1989), 2nd ed.
[38] J. E. Marsden and T. Ratiu, *Introduction to Mechanics and Symmetry* (Springer-Verlag, New York, 1994).
[39] F. J. Sacherer, IEEE Trans. Nucl. Sci. **18**, 1105 (1971).